New Zealand Fisheries
Assessment Report
2009/23
April 2009
ISSN 1175-1584

The 2008 stock assessment of rock lobster (*Jasus edwardsii*) in CRA 3

Paul A. Breen
Vivian Haist
Paul J. Starr
Terese H. Kendrick

The 2008 stock assessment of rock lobster (*Jasus edwardsii*) in CRA 3

P. A. Breen[1]
V. Haist[2]
P. J. Starr[3]
T. H. Kendrick[4]

[1]NIWA
Private Bag 14901
Wellington 6241

[2]1262 Marina Way
Nanoose Bay
British Columbia, Canada V9P 9C1

[3]161a Rhine Street
Wellington 6023

[4]Trophia
P O Box 60
Kaikoura 7340

New Zealand Fisheries Assessment Report 2009/23
April 2009

Published by Ministry of Fisheries
Wellington
2009

ISSN 1175-1584

Breen, P.A.; Haist, V.; Starr, P.J.; Kendrick, T.H.; (2009).
The 2008 stock assessment of rock lobster (*Jasus edwardsii*) in CRA 3.
New Zealand Fisheries Assessment Report 2009/23. 54 p.

This series continues the informal
New Zealand Fisheries Assessment Research Document series
which ceased at the end of 1999.

EXECUTIVE SUMMARY

Breen, P.A.; Haist, V.; Starr, P.J.; Kendrick, T.H. (2009). The 2008 stock assessment of rock lobster (*Jasus edwardsii*) in CRA 3.

***New Zealand Fisheries Assessment Report 2009/23.* 54 p.**

This document describes the stock assessment of CRA 3 made in 2008. A companion report describes the data and the model used for the assessment. This document describes the specifications for the base case assessment, results from the mode of the joint posterior distribution (MPD), MPD sensitivity trials, the Markov chain – Monte Carlo (McMC) results, forward projections and assessment results. A procedure for calculating the indicators *MSY* and *Bmsy* is described.

The assessment was disrupted by the discovery that a shift has occurred in CRA 3 lobster growth, as seen in older and new tag-recapture data. This required a change to the model that took up a substantial part of the allotted time. McMC diagnostics were not very good, although the Plenary accepted the assessment. The assessment suggests a depleted stock, just above *Bmin* and well below *Bmsy*.

1. INTRODUCTION

This document describes the stock assessment of CRA 3 conducted in 2008. The stock assessment was done under Objective 4 of Ministry of Fisheries (MFish) contract CRA2006/01, a three-year contract awarded to the New Zealand Rock Lobster Industry Council Ltd. (NZRLIC). In New Zealand there are nine rock lobster stocks, not all of which can be assessed each year. The choice of stock to assess was made by the National Rock Lobster Management Group (NRLMG). The stock assessment was guided by the Rock Lobster Fishery Assessment Working Group (RLFAWG).

The CRA 3 stock extends from East Cape south to the Wairoa River. The TACC is distributed amongst 39 quota share owners, with significant iwi involvement in quota share ownership and fishing. In the 2007–08 fishing year, CRA 3 landings were reported by 28 commercial vessels. The commercial harvest has an approximate landed value of $8.1 million (based on an average port price paid to fishermen). There are two processing plants in Gisborne, and product is also shipped to Wellington, Tauranga and Auckland for processing and export (NRLMG 2008).

The stock assessment was conducted with a multi-stock length-based model (MSLM) that was purpose-built for lobster stock assessments (Haist et al. 2009). For the CRA 3 stock assessment, the model was used as a single-stock model. This model was driven by catch estimates and assumptions, two abundance indices, length frequency data from observer catch sampling and voluntary logbooks, tag-recapture data and a puerulus settlement index.

Because of the complexity of this stock assessment, the documentation has been divided into two publications: a companion document (Starr et al. 2009) describes the model and data, and this document, describing fitting the model to data, the Markov chain – Monte Carlo simulations, forward projections and assessment results.

An important feature of the assessment was an apparent regime shift in growth. Exploratory analyses of the tag-recapture data showed that growth rates estimated from an older set of data, from 1975 through 1981, were much greater than those from data collected from 1995 through 2006. An independent study confirmed the slow growth in the recent data series. To address this, the assessment team explored and reported to the RLFAWG two approaches. The first required a substantial change to the assessment model and involved fitting to both tag-recapture data sets; estimating growth parameters separately for the two periods and estimating transitional growth rates for 1982–94. The second approach was to fit only to the data from 1982 onwards, ignoring the earlier period with demonstrably faster growth.

Both approaches were reported to the RLFAWG, but the second approach had problems that caused its results to be rejected. Only the first approach will be described here.

The document refers to two seasons: autumn-winter (AW), from 1 April through 30 September, and spring-summer (SS), from 1 October through 31 March. The rock lobster fishing year extends from 1 April through 31 March. Where a fishing year is referred to by a single year, the year is the April-December calendar year portion of the fishing year; *viz.* "2003" refers to the 2003–04 fishing year. Minimum legal size is abbreviated as MLS; tail width (the measurement on which MLS is based) as TW; the size-limited catch and fishery are designated SL and the non-size-limited catch and fishery are designated NSL; autumn-winter and spring-summer seasons are designated AW and SS, respectively; the mode of the joint posterior distribution is termed the MPD and Markov-chain – Monte Carlo simulation is called McMC; sdnr is the standard deviation of the normalised residuals and MAR is the median of absolute normalised residuals.

2. MPD RESULTS

2.1 Specification of the base case

The base case was chosen after c. 100 exploratory runs had been made with the version that was finally accepted, and an equal number with the alternative version that ignored the early data. These runs explored the effects of starting the model at a later time, fixing some parameters in various combinations and at different values, and changing the weights used for different datasets, using different model options.

The base case was fitted to all datasets except the puerulus settlement index. A section below describes a focused study of the utility of that index. We discovered that the 1986 length frequency data gave very large residuals, and this one record was excluded from the analyses.

The MSLM model was used as a single-stock model. The movement option was therefore not used. Density-dependent growth and stock-recruitment options were not used. The growth model option was the Schnute model, and the selectivity curve option was the double-normal. The dynamics option was instantaneous, using direct estimate of mortalities by fitting to catches.

Model quantities discussed in this report are defined in Table 1. Some specifications of the model for the base case are shown in Table 2. The model was run from 1945 through 2007 (using data to the end of March 2008), estimating an *Rdev* for each year through 2004 (after which there was considered to be no signal in the data).

The major model change – estimating two sets of growth parameters from the two tag datasets – required a change in the size of the initial bin. In previous assessments, the smallest bin was 30 mm. However, this is well below the size represented by the tag-recapture data, and initial results from estimating two sets of growth parameters showed, in the second set of estimates, smaller growth in larger fish but faster compensating growth in the small sizes. We did not consider this model response to be credible, especially without corroborating observations from data. After exploring and testing three possible approaches, we fixed the problem by increasing the smallest bin to 44 mm.

The model's marine reserve option was used, with the Te Tapuwae o Rongokako marine reserve near Gisborne starting in 1999 and assumed to be alienating 10% of the lobster habitat in CRA 3.

Table 3 shows the switches, likelihoods and weights for the various datasets. The puerulus index was not fitted. Multinomial likelihood was used for LFs, robust normal for tag-recaptures and lognormal for all other datasets.

The handling of estimated parameters (ignoring those related to unused model options) is shown in Table 4. The initial exploitation rate parameter *InitER* was fixed at zero because the model was started in 1945, at the beginning of significant fishing on this stock. The puerulus index was not fitted, so *qpoo* was not estimated. The shape parameter *CPUEpow* was left at 1 in the base case. The maturity parameters were fixed at values given from an external analysis of the LF data, because the model had a tendency to make estimates on the lower bounds. The signal is weak for maturation because of the early onset of maturity in CRA 3 and the consequent small number of immature female LF samples in the data, so these parameters are hard to estimate (and don't have much effect on results).

GrowthCV was fixed to produce a positive definite Hessian. The minimum standard deviation of growth *MinStd*, the observation error *GObs*, and the right-hand limb of selectivity *varR*, were all fixed according to long usage.

Fixed quantities are shown in Table 5. The LF data were explored outside the model to determine the range of size bins for each sex that contained most of the data, and the model used this range in fitting, treating the smallest bin in the range as a minus group and the largest as a plus group. This prevented the model from having to fit to a large number of very small proportions at small and large sizes outside the range of data, which distorts the residuals. The bins used are shown in Table 5.

2.2 Base case MPD results

MPD estimates from the base case are shown in Table 6. The normalised residuals were not perfectly balanced: for instance, the CPUE dataset was intentionally over-weighted, giving an sdnr greater than 1 and MAR greater than 0.67. Note that these indicators are rough guides: for LFs, the sdnr was much greater than 1, suggesting too much weight, while the MAR was only 0.51, suggesting that more weight was required.

M was estimated at 0.165. While greater than the mean of the prior (0.12), this is far lower than estimates obtained in the previous assessment (Breen et al. 2005). In that assessment, the regime shift in growth had not been detected (substantially fewer tag-recapture records were available from 1995 and later), so the model was trying to reconcile the length frequencies and the relatively fast growth from the older tag data by making *M* high. Our detection of the regime shift has solved that problem.

The fit to CPUE was generally good (Figure 1) The predictions were lower than observed for SS in years 1996–99, but these were years with little fishing in the SS because of the high abundance and high catches in AW.

Although the CR dataset was under-weighted, the fit was good (Figure 2). Fits to the LF data were generally good (Figure 3) if one remembers that immature females were very low in proportion to the total. QQ plots of the residuals are shown in Figure 4 and the residuals are summarised by sex, size and season in Figure 5.

Fits to the tag-recapture data are shown in Figure 6, Figure 7 and Figure 8. The predicted growth curves for the two periods are shown in Figure 9: growth was estimated to be much greater based on the 1975–81 tags than for the 1995–2004 tags.

The initial length structure is shown in Figure 10. Males show a substantial accumulation in the last bin, but we know from previous explorations that this disappears rapidly at the onset of fishing. The predicted mode of females is well below the MLS.

The MPD recruitment trajectory is shown in Figure 11. For some reason the model estimates low recruitment for the years before 1979, when the CPUE data series begins. After that year, the model estimates a period of high recruitment from the late 1970s to the early 1980s, another period of high recruitment in the early 1990s, and much lower recruitment after 1991.

The estimated trajectory of vulnerable biomass (Figure 12) is similar for both seasons. It shows a steady decline to the early 1990s, a strong increase to a peak in 1998, then a decline to current levels not far above the minimum biomass attained in the 1990s. The recruited biomass trajectory by sex is shown in Figure 13.

Exploitation rate is shown in Figure 14. The model estimates that the SL fisheries are much more important than the NSL, and that exploitation rate was high in the 1980s and early 1990s, decreased to low levels in the mid to late 1990s and has increased again since then.

Estimated surplus production is plotted against recruited biomass in Figure 15. This shows a slow increase until 1979 as biomass declined, a sharp increase to the mid 1980s and subsequent decline.

2.3 MPD sensitivity trials

The first group of trials examined the effect of changing the transition between the periods of fast and slow growth. In the base case the transition runs from 1982 through 1994. Three trials were done, with a quick transition occurring after 1981–82 or after 1994–95 and a slow transition from 1985 through 1990. These trials and their names are 1) 1981–82, 2) 1994–95 and 3) 1985–90. Thus the base case has a gradual transition occupying the whole period between 1981 and 1995; the trials have a sharp transition at the early end and at the late end, and a shorter middle transition.

The second group of trials altered the model's assumptions. Seven trials were done:

4) using finite instead of instantaneous dynamics (finite),
5) estimating *CPUEpow* to allow a non-linear relation between CPUE and biomass (CPUEpow),
6) estimating *GrowthCV* (GCV),
7) estimating *varR* to allow for domed selectivity (domed),
8) fixing $M = 0.12$ (fixM),
9) estimating the maturity parameters mat50 and mat95 (estmat) and
10) fixing SelMaxF in both epochs at the MLS of 60 mm (SelMaxF60).

The third group changed the treatment of NSL catches, which are poorly determined. Trial 11 used a high CV when estimating NSL exploitation rate parameters (hiCVCnsl), which allowed the model to reduce the closeness of the fit to the NSL catches. Trial 12 estimated the scalar multiplier for NSL catches (scalarCnsl), allowing the model to change the NSL catch to obtain best fit to the remaining data. In Trial 13 we reduced the estimated illegal catch by 50% from 1990 forward (halfillegal).

In the fourth group, Trial 14 explored the effect of ignoring the marine reserve (noMR).

In the fifth group, six trials explored different starting years and assumed *InitER*:

15) start year = 1963, *InitER* = 0.1 (start63.1),
16) start year = 1963, *InitER* =0.4 (start63.4),
17) start year = 1963, *InitER* =0.7 (start63.7),
18) start year = 1974, *InitER* =0.1 (start74.1),
19) start year = 1974, *InitER* =0.4 (start74.4) and
20) start year = 1974, *InitER* =0.7 (start74.7).

In the sixth group of trials, we removed datasets from the fitting one at a time. Trials 21 through 23 removed the LF, tag-recapture and CPUE data respectively.

For these trials, *MSY* and *Bmsy* were calculated as described by Starr et al. (2009) and described below (see Section 4.1). *Bref* was calculated as the mean AW vulnerable biomass from 1974 through 1979. For other indicators see the discussion in the "Forward projections" section below.

In the trials 1–3, with altered transitions between the two growth regimes, none of the fits was better than in the base case (Table 7). Most of the difference in function value was due to differences in the CPUE likelihood, except for trial 2, where the fit to CPUE was better but the fit to LFs was worse. Differences in growth parameters and other parameters were minor. Estimated current biomass was less in trial 2. The most substantial difference in this group was that *MSY1* and *MSY2* were much smaller than the base case in all three trials.

In the second group, using finite dynamics (trial 4, Table 7) gave a worse fit, especially to the LFs, as was seen by Haist et al. (2009). Estimating *CPUEpow* in trial 5 gave nearly the same fit: the estimated value of 1.03 reflects very slight hyperstability. However, the estimated *Bref*, *Bmsy* and associated parameters all differed substantially from the base case, suggesting that these are not well determined.

Estimating *GrowthCV* in trial 6 also improved the fit. For males in the first period and females in the second, the estimated *GrowthCV* was only slightly higher than the assumed base case value; for males in the second period and females in the first, *GrowthCV* nearly doubled. Both *MSY* values were much smaller than in the base case.

Estimating the right-hand limb of selectivity in trial 7 improved the fit substantially, with improved contributions from tags, LFs and CPUE. For both males and females in both epochs, *SelMax* went to small values: three of the four estimates were smaller than associated *varL* estimates. These low values allowed the model to fit declining proportions-at-length for larger fish with estimated *M* that was close to the prior mean. Estimated current biomass was similar to the base case value, but *Bref* and *MSY* were much larger.

In trials 8 through 14 (Table 8), fixing parameters (*M* in trial 8 and *SelMaxF* in trial 10) gave worse fits than the base case; conversely, estimating previously fixed parameters gave better fits. Ignoring the marine reserve gave nearly the same fit. Growth parameters showed little difference, but *vuln2* and *vuln3* showed sensitivity, especially in trial 10. *Bref* and *Bcurr* showed relatively small variation, but *MSY1* showed large variations across these trials. Note also that the F multiplier associated with *MSY2*, which was 1.2 in the base case, became less than 1 in three of the trials. The base MPD suggested that the optimum fishing mortality rate was higher than current, while these trials suggested the current rate was higher than optimal.

In trials 15 through 20, exploring different model starting places (Table 9), later starts tended to fit the data better, and higher assumed *InitER* also fitted the data better. The best fit was in trial 20, with a 1973 start and initial exploitation rate of 70%. Assumed *InitER* of 0.1 gave worse fits than in the base case. *Bref* was similar across these fits except for trial 18, a possible convergence problem. *Bmsy1* showed great variation across the trials, but *Bmsy2* and both *MSY* estimates did not vary much.

When datasets were removed in trials 21 through 23 (Table 9), the pattern of likelihoods was as expected: for instance, removing LFs resulted in a better fit to tags and CPUE. The fit to CR did not change much except that it increased 3 points when CPUE was removed. The *Galpha*

parameters in trial 22, with no tags, were not much different from the base case values, but *GBeta* values for the first period were much less. Growth parameters from the second period were all similar to the base case, suggesting strong information about growth in the CPUE and LF data. Estimated selectivity parameters were not sensible when LFs were removed. Many of the biomass and *MSY* indicators were little changed from the base case, again suggesting high redundancy in these datasets.

Figure 16 shows the indicator ratio *Bcurr/Bref* plotted against *Bref* for the base case and 15 of these trials. The GCV trial has much higher *Bref* and lower ratio than the base case, and the domed trial also lies away from the pack, but the remainder of the trials are near the base case values.

Figure 17 shows the indicator ratio *Bcurr/Bmsy2* plotted against *Bmsy2* for the base case and 15 of these trials. Again, GCV trial is an outlier with low Bmsy2 and high ratio, while the domed trial lies away from the pack in the other direction.

Figure 18 shows the indicator ratio *Bcurr/Bref* plotted against *Bref*. In this plot, most of the variation is in current biomass, with little in the ratio except for start73.1 (a low ratio) and start63.7 (a high ratio).

The trials suggest that the MPD results are somewhat sensitive to some of the modelling choices made. Assessment indicators were sensitive to the choice of growth transition period between the two regimes. The finite trial confirms that the instantaneous dynamics option is the better choice. Estimating *CPUEpow* gave what appeared to be only a slightly different fit, but indicators were changed substantially, suggesting these are not well determined. The GCV trial confirmed that the *GrowthCV*s should be estimated if possible (it was not possible to find a useable base case that could be taken to the McMC stage when these were estimated). While better fits to the data were obtained when starting the model later than 1945, we found that it was not possible to estimate the *InitER* parameter.

The domed trial shows that the model would like to estimate strongly domed selectivity, allowing it to create a cryptic population of large fish. It is not safe to base an assessment on this approach, especially when the prices for larger grades have high differentials and there is a strong incentive to catch larger fish, making domed selectivity unlikely.

3. McMC RESULTS

The McMC simulation was started at the base case MPD and run for 3 million simulations with every thousandth sample saved, giving a set of 3000 samples. For diagnostics we used first, the trace for each parameter and second, a plot of the running median and 5th and 95th quantiles, and the moving average over 40 samples. These were examined to establish that the traces appeared stable and well mixed and that the chains appeared to have converged.

The number of parameters was 282, and we produced a trace and a diagnostic plot for each estimated parameter as well as plots for a selection of derived parameters. We show these for only a small proportion of parameters, but we believe the selection is representative.

Traces varied in quality. The *Rdevs* showed generally good mixing and stability – Figure 19 shows some early ones, as well as the major parameters *lnR0* and *M* and the objective function value. Figure 23 shows the diagnostic plots for these eight quantities, all showing acceptable

stability except that the moving mean for *M* has a late excursion. Figure 20 and Figure 24 show traces and diagnostics, respectively, for the last *Rdev*, the two catchability coefficients *lnqCPUE* and *lnqCR*, and some growth parameters. The trace for *lnqCPUE* is not very well mixed, although the diagnostic plot suggests convergence by the end of the run. The *lnqCR* trace shows a steady upward trend through the run, and does not show acceptable convergence.

This problem is also seen in the estimated fishing mortality rates in Figure 21, Figure 22, Figure 25 and Figure 26, where the traces show a trend and the running medians and moving means have not stabilised by the end of the run.

These diagnostics are not good, and they create uncertainty in the assessment results. If there had been time to do so, we would have made a much longer McMC run.

Posterior distributions from these examples are shown in Figure 27 through Figure 30. Note that the MPD estimates are well outside the weight of the distributions for the catchability coefficients, some growth parameters and the mortality rates. This result calls into question the utility of the MPD sensitivity trials. Marginal posterior distributions for some key parameters are summarised in Table 10.

The posterior distribution of predicted CPUE is shown in Figure 31 and the fit to CR in Figure 32. These are similar to the MPD fits (*see* Figure 1 and Figure 2). The posterior distributions of *Rdev*s are shown in Figure 33: the same trend is seen as in the MPD (*see* Figure 11). The figure includes projected *Rdev*s: projections are discussed below.

The seasonal trajectories of vulnerable biomass are shown in Figure 34 and SL exploitation rate in Figure 35, again including the projections. Surplus production is shown in Figure 36.

4. FORWARD PROJECTIONS

4.1 Methods

The last year of the fitted model was 2007, but the model calculates the initial biomass for the following season, AW 2008, for use as current biomass. We made 5-year projections through 2012 from the set of 3000 samples of the joint posterior distribution of parameter estimates. In these projections, catches were assumed to remain constant at their 2007 values, except that the TACC of 190 t was used for commercial catch (this was about 20 t greater than the 2007 commercial catch). The 2007 commercial catch seasonal split was used.

Recruitment (the *Rdev*s) was re-sampled from the most recent ten years of estimates: – 1995–2004. The minimisation model used the 2004 *Rdev* estimate for 2005–2007, but the projection model used randomly resampled estimates for these years and re-ran the dynamics from 2005 onwards. These projections are sensitive to the period chosen from which to re-sample recruitment, because recruitment trends are different over different periods (see Figure 33). The most recent 10 years of estimates are considered the best information about likely future recruitments in the short term.

Indicators were discussed by the RLFAWG but were revisited by the Plenary and the NRLMG. The indicators reported here are those agreed by the Plenary or requested by the NRLMG, not those originally reported to the RLFAWG. Biomass indicators are based on beginning of season AW vulnerable biomass, which is the biomass legally and functionally available to the fishery,

taking MLS, female maturity, selectivity-at-size and seasonal vulnerability into account.

The limit indicator *Bmin* was defined as the nadir of the vulnerable biomass trajectory (using current MLS), 1945–2007; current biomass, *B2008*, was defined as the initial vulnerable biomass in AW 2008; projected biomass, *B2012*, was defined as the initial vulnerable biomass in AW 2012.

A biomass indicator associated with *MSY* or maximum yield, *Bmsy*, was calculated for each sample of the joint posterior as follows. Forward projections were made for 50 years, using the mean of *Rdevs* from 1979 through 2004. This range of years was chosen because they represented the period during which the model had estimated recruitments from adequate data, and were considered the best available information about likely long-term average recruitment. These *MSY* and *Bmsy* calculations are sensitive to the period chosen to represent the mean recruitment, which varied substantially over the model reconstruction period (see Figure 33). Varying the period used to represent mean recruitment would cause considerable variation in estimated *Bmsy*.

The projections used to estimate *MSY* and *Bmsy* were based on the growth parameters estimated from the second (1996–2006) tag dataset. Estimated *MSY* and *Bmsy* would be different if growth rates from the earlier (1975–81) dataset were used. The Plenary agreed that it was more appropriate to base these calculations on the estimates of current growth.

When estimating *MSY* and *Bmsy*, it was agreed to hold the NSL catches (customary and illegal) constant at their assumed 2007 values and to vary the SL fishery mortality rate *F* systematically across a range of values, making a 50-year projection for each *F* value. To obtain the range of *F* values, the model applied a set of multipliers ranging from 0.1 to 2.5 to the AW and SS *F* values that had been estimated for 2007 for the SL catch for each of the 3000 samples from the joint posterior distribution. The model used a Newton-Raphson algorithm to find the NSL fishery mortality rates.

The model then inspected the annual (AW plus SS) SL catches from this set of projections, took the maximum to be *MSY* and recorded the associated AW biomass as *Bmsy*. If the *MSY* was still increasing with the highest *F* multiplier, the *MSY* and *Bmsy* obtained with that multiplier were used. The multiplier that produced *MSY*, *Fmult*, was also reported as an indicator.

Additional reported indicators were the exploitation rate associated with the SL catch from 2007 and 2012: *USL2007* and *USL2012* respectively. At the request of the NRLMG, we also compared projected CPUE with an arbitrary target of 0.75 kg/potlift.

As well as indicators described above, we calculated various ratios for each of the 3000 samples, for instance *B2008/Bmsy*. The assessment was based on the medians of posterior distributions of the indicators, and medians of the posterior distributions of indicator ratios. We also calculated probabilities for selected propositions: for instance, the probability that current biomass was less than *Bmin* – P(*B2008*<*Bmin*) – was calculated by inspecting the 3000 forward projections to determine the percentage in which the proposition was true.

At the request of the NRLMG, we calculated whether CPUE in AW 2012 (*CPUE2012*) exceeded the arbitrary reference value of 0.75 kg/potlift for each sample. CPUE in AW 2012 was calculated from the vulnerable biomass in AW 2012 and the estimate of *lnqCPUE*.

As well as projections with the current level of catches, the NRLMG requested additional projections where the SL catch was reduced to 90%, 80%, 70%, 60%, 40%, 20% and 0% of the value described above.

4.2 Results

Projections made with current catch levels, using the TACC for projected commercial catch, are summarised in Table 11. Current biomass *B2008* was above *Bmin* in 83% of runs, and the median result was 11% above *Bmin*. Current biomass was above *Bmsy* in less than 1% of runs, and the median result was half *Bmsy*. Current exploitation rate was about 55%.

In the five-year projections, biomass increased in only 25% of projections; the median result was a decrease of 25%. Projected biomass *B2012* had a median of 124 t, but uncertainty around this was high, with a 5% to 95% range of 65 to 256 t. *B2012* was above *Bmin* in 36% of runs, and the median result was 83% of *Bmin*. *B2012* was greater than *Bmsy* in less than 1% of runs, and the median was 37% of *Bmsy*.

Projected CPUE had a median of 0.5 kg/potlift, and only 20% of runs exceeded 0.75 kg/potlift. The mean *F* multiplier associated with *MSY* was 0.73, suggesting that *Fmsy* is lower than the 2008 level.

These results suggest a stock that is near *Bmin* and well below *Bmsy*. Under current catches and TACC, and using recent recruitment patterns, the model predicted a 75% probability of biomass decrease over four years.

Results from alternative catches are shown in Table 12. Projected biomass and CPUE obviously increase as the projected catches decrease, and the probability that biomass will exceed a reference also increases. These results were used by the NRLMG in forming its advice to the Minister of Fisheries in December 2008 (NRLMG 2008).

5. DISCUSSION

The conduct of this assessment was greatly changed when we discovered that growth implied by tag-recapture data changed at some point between an earlier period of data (1975–81) and a later period (1995–2006) (*see* Starr et al. (2009)). This discovery caused us to re-write the model so that two sets of growth parameters were estimated (for this also, see Starr et al. 2009), which used up some of the allotted time that might have been spent elsewhere. An alternative approach was attempted that involved starting the model after 1981 and estimating the *InitER* parameter, but McMC diagnostics and other results were sufficiently poor to cause the RLFAWG to reject this approach.

A generic change to the model allowed us to use instantaneous dynamics in the base case. Previously, the model estimated fishing mortality rates from biomass and catch with an iterative loop. This worked well but was far too slow to be practical (Haist et al. 2009). Estimating these rates directly by fitting to catch added a great number of estimated parameters to the model, but this modification did not slow processing very much and appeared to work well. Both the Haist et al. (2009) assessment and the present assessment showed that fits were better when using instantaneous dynamics.

There were some difficulties fitting the model to the data. We were forced to fix the *GrowthCV* parameters to obtain a positive definite Hessian matrix, and these were parameters we would have preferred to estimate. We experienced difficulties when we attempted to start the model in the 1960s or 1970s with estimated *InitER*. Because results were sensitive to an assumed *InitER* (see the MPD sensitivity trials), we thought it best to start in 1945 with *InitER* = 0.

The estimated recruitment trajectory (*see* Figure 12 and Figure 33) resulting from the 1945 start appears distinctly odd: recruitment was lower than average and declining until 1979, then it increased 3- or 4-fold for a time, and declined from there. The pre-1979 estimates were based only on the catch and CR data, and were not considered robust enough to use in *Bmsy* calculations.

The McMC simulations did not have good diagnostics: had time permitted, we would have run a much longer chain over a week. Besides having poor diagnostics, the McMC results for several quantities were well removed from the MPD estimates. This casts some doubt on the utility of MPD sensitivity trials. Again, had time permitted, we would have followed the usual practice of running a set of McMC sensitivity trials.

This assessment is the first in which we have calculated *MSY* and *Bmsy* with a Bayesian length-based model. Any such calculation requires an assumption about the average level of recruitment, with higher average recruitment implying higher *Bmsy* and *MSY*. It is obvious from inspection of Figure 33 that these estimates will be sensitive to the period chosen to represent average recruitment. The mean of *Rdev*s ending in 2004 and beginning from any previous year is shown in Figure 37. There is a low point when 2001–2004 is sampled, following which the average recruitment increases as more years are sampled, reaching a peak when 1978–2004 are sampled. Sampling years before 1978 causes the mean recruitment to decrease again, and the lowest point of the series occurs when the full range of years (1945–2004) are sampled.

Thus *Bmsy* and *MSY* will be sensitive to the period chosen to represent average recruitment, which is an arbitrary decision. They will also be sensitive to how the NSL catches are handled (also arbitrary in the absence of good data). We assumed that these catches remained constant, but a plausible alternative assumption is that they are proportional to abundance. We based *Bmsy* on AW vulnerable biomass. This is also an arbitrary choice: it could be based on SS biomass, or on an average of the two seasons; *Bmsy* might alternatively be based on total biomass or mature biomass. The calculation of *MSY* and *Bmsy* indicators requires further discussion and investigation before they can be fully useful to management.

These sources of uncertainty in the conclusions relative to *MSY* and *Bmsy* should be borne in mind when considering the assessment results.

The forward projections suggest that the stock is probably above *Bmin*, although not very far above, and is well below the estimated *Bmsy*. Under current levels of non-commercial catches and the current (2008–09) TACC, and with levels of recent (1995–2004) recruitment, the stock is projected to decrease. Current fishing mortality rate is approximately 27% higher than *Fmsy*.

6. ACKNOWLEDGMENTS

This project was conducted under New Zealand Ministry of Fisheries contract CRA2003/01, awarded to the New Zealand Rock Lobster Industry Council Ltd. We thank Nito Dano and Afa Logovae for logistic support, Daryl Sykes for advice and encouragement, and Andre Punt for his helpful discussion of *Bmsy*.

7. REFERENCES

Breen, P.A.; Kim, S.W.; Haist, V.; Starr, P.J. (2005). Management procedure evaluations for rock lobsters in CRA 3 (Gisborne). *New Zealand Fisheries Assessment Report 2005/61*. 71 p.

Haist, V.; Breen, P.A.; Starr, P.J. (2009). A new multi-stock length-based assessment model for New Zealand rock lobsters (*Jasus edwardsii*). *New Zealand Journal of Marine and Freshwater Research 43(1)*: 355-371.

National Rock Lobster Management Group. (2008). Annual Report to the Minister of Fisheries, Hon. Phil Heatley. Unpublished report, Wellington. 139 p. + 2 Annexes.

Starr, P.J.; Breen, P.A.; Kendrick, T.H.; Haist, V. (2009). Model and data used for the 2008 stock assessment of rock lobsters (*Jasus edwardsii*) in CRA 3. *New Zealand Fisheries Assessment Report 2009/22*. 62 p.

Table 1: Definitions of some model quantities, using their informal names.

Quantity	Definition
lnR0	natural log of base recruitment
initER	initial equilibrium exploitation rate
M	instantaneous rate of natural mortality
Rdev	annual recruitment deviations acting in log space
sigmaR	standard deviation of recruitment deviations
lnqCPUE	natural log of catchability for the CPUE data
lnqCR	natural log of catchability for the CR data (historical abundance index)
qPoo	scalar between puerulus settlement index and model recruitment
CPUEpow	shape parameter for CPUE vs biomass
mat50	size at which 50% maturation occurs
mat95	size at which 95% maturation occurs
Galpha	expected growth at 50 mm TW; *GalphaM* and *GalphaF* for males and females
GBeta	expected growth at 80 mm TW (derived)
Gdiff	*GBeta = Galpha * Gdiff*
Gshape	shape parameter for expected growth vs initial length
GrowthCV	CV of expected increment
MinSD	minimum standard deviation of expected growth increment
GObs	observation error standard deviation for tag-recapture data
SelMax	size at maximum selectivity
varL	shape of selectivity curve to the left of *SelMax*
varR	shape of selectivity curve to the right of *SelMax*
vuln1	relative seasonal vulnerability of males in AW
vuln2	relative seasonal vulnerability of immature females in AW
vuln3	relative seasonal vulnerability of all females in SS
vuln4	relative seasonal vulnerability of mature females in AW
Cnsl_scaler	scale parameter for assumed and actual NSL catches

Table 2: Model specifications for the base case.

StartYear	EndYear	First Rdev	Last Rdev
1945	2007	1945	2004
First Year with two seasons	1974		
Last Year for tag dataset 1	1981		
First Year for tag dataset 2	1995		
Lefthand edges of first bin (mm)	44		
Lefthand edge of last bin (mm)	90		
Bin width (mm)	2		
Mean size at recruitment	46		
Std. dev. of size at recruitment	2		
Marine reserve start date	1999		
Marine reserve proportion	0.1		

Table 3: For each dataset, the base case switch (0 or 1 = on or off), likelihood (2 = lognormal, 3 = multinomial, 7 = robust normal) and relative weight.

Dataset	LFs	Tag	CPUE	CR	Puerulus
switch	1	1	1	1	0
likelihood	3	7	2	2	2
weight	23	1.15	1.5	1	1

Table 4: For estimated parameters in the base case: estimation phase (negative = fixed), lower and upper bounds, prior type (0 = uniform, 1 = normal, 2 = lognormal), prior mean and CV, and initial value. Shading indicates fixed parameters. Parameters are not shown for model options that were not used, such as movement.

Parameter	Phase	LB	UB	Prior	Mean	CV	Initval
lnR0	1	1	25	0	-	-	14
InitER	-2	0	0.99	0	-	-	0
M	5	0.01	0.35	2	0.12	0.4	0.2
Rdev	3	-2.3	2.3	1	0	0.4	0
lnqCPUE	1	-25	0	0	-	-	-6
lnqCR	1	-25	2	0	-	-	-3
qPoo	-1	-25	0	0	-	-	-6
CPUEpow	-1	0.001	2	0	-	-	1
mat50:	-6	30	80	0	-	-	39
mat95:	-6	5	80	0	-	-	14
Galpha	2	0.1	20	0	-	-	3
Gdiff	2	0.001	1	0	-	-	0.5
Gshape	2	0.1	15	0	-	-	6
GrowthCV	-4	0.01	5	0	-	-	0.5
MinSD	-2	0.01	5	0	-	-	1.5
Gobs	-1	0.00001	10	0	-	-	1
varLM	5	1	50	0	-	-	8
varLF	5	1	50	0	-	-	10
varRM	-3	1	250	0	-	-	200
varRF	-3	1	250	0	-	-	200
SelMaxM	4	30	70	0	-	-	54
SelMaxF	4	30	80	0	-	-	60
vuln1	3	0.01	1	0	-	-	0.8
vuln2	3	0.01	1	0	-	-	0.01
vuln3	3	0.01	1	0	-	-	0.4
vuln4	3	0.01	1	0	-	-	0.12

Table 5: Fixed quantities used by the base case.

Quantity	Value	
sigmaR	0.4	
CPUE process error	0.25	
CR relative sigma	0.3	
handling mortality	0.1	
fishing dynamics	instantaneous	with estimated mortalities
growth model	Schnute	
selectivity	double normal	
selectivity epochs	2	
epoch change	1993	
maximum vulnerability	males in SS	
first bin for fitting LFs (mm)	44	
largest LF bin (males, mm)	76	
largest LF bin (immature females, mm)	60	
largest LF bin (mature females, mm)	76	
length-weight	a	b
male	4.16E-06	1.30E-05
female	2.9354	2.5452

Table 6: Estimates from the base case MPD. For the datasets, sdnr is the standard deviation of the normalised residuals; MAR is the median of the absolute residuals, LL is the likelihood contribution. Fixed parameters are not shown. For growth parameters, the number represents the earlier or later tag dataset; for selectivity parameters, the number refers to the epoch.

Quantity	Value
LF dataset–sdnr	1.76
LF dataset–MAR	0.51
LF dataset–LL	1137.4
Tag dataset–sdnr	1.36
Tag dataset–MAR	0.71
Tag dataset–LL	7395.1
CPUE dataset–sdnr	1.27
CPUE dataset–MAR	0.83
CPUE dataset–LL	-20.4
CR dataset–sdnr	0.350
CR dataset–MAR	0.183
CR dataset–LL	41.3
Catch data–LL	1.0
Contributions from priors	4.9
Total function value	8560.3
lnR0	13.62
M	0.165
lnqCPUE	-6.00
lnqCR	-3.42
GalphaM1	4.39
GBetaM1	4.36
GdiffM1	0.99

Quantity	Value
GshapeM1	6.75
GalphaF1	1.51
GBetaF1	1.35
GdiffF1	0.90
GshapeF1	15.00
GalphaM2	2.34
GBetaM2	1.97
GdiffM2	0.84
GshapeM2	15.00
GalphaF2	1.12
GBetaF2	0.56
GdiffF2	0.49
GshapeF2	0.10
1vulnest	0.826
2vulnest	0.390
3vulnest	1.000
4vulnest	0.321
varL1M	4.589
SelMax1M	53.49
varL1F	8.05
SelMax1F	65.21
varL2M	5.98
SelMax2M	54.47
varL2F	8.77
SelMax2F	68.04

Table 7: Results from the first two groups of MPD sensitivity trials, with the base case in the first column.

	base case	Alter treatment of growth transition period			Change model estimation assumptions			
Trial number		1	2	3	4	5	6	7
Trial name		1981-82	1994-95	1985-90	finite	CPUEpow	GCV	domed
Total function value	8556.7	8578.3	8588.3	8566.9	8604.4	8556.6	8510.4	8484.8
LFs-sdnr	1.76	2.09	1.64	1.82	1.80	1.74	1.72	1.99
LFs-MAR	0.51	0.51	0.52	0.50	0.51	0.50	0.49	0.47
LFs-LL	1136.4	1134.4	1191.6	1135.4	1187.6	1137.1	1133.4	1114.9
Tags-sdnr	1.36	1.37	1.39	1.37	1.36	1.36	1.19	1.36
Tags-MAR	0.71	0.72	0.71	0.72	0.71	0.71	0.66	0.70
Tags-LL	7392.4	7402.2	7395.2	7404.4	7386.1	7392.6	7347.4	7377.8
CPUE- sdnr	1.29	1.43	1.02	1.39	1.39	1.28	1.32	1.39
CPUE-MAR	0.83	0.92	0.68	0.84	0.97	0.86	0.86	0.85
CPUE-LL	-18.6	-7.9	-36.9	-11.2	-11.5	-19.7	-16.9	-11.3
CR-sdnr	0.35	0.35	0.34	0.35	0.35	0.35	0.35	0.49
CR-MAR	0.18	0.18	0.22	0.17	0.18	0.18	0.18	0.33
CR-LL	41.3	41.3	41.3	41.3	41.3	41.3	41.3	41.9
Catch-LL	0.9	1.1	0.9	1.1	0.0	0.9	1.0	0.7
Prior contributions	4.2	7.3	-3.8	-4.1	0.8	4.3	4.2	-39.2
lnR0	13.6	13.7	13.7	13.7	13.6	13.6	13.6	13.9
M	0.16	0.17	0.17	0.17	0.16	0.16	0.16	0.11
InitER	0*	0*	0*	0*	0*	0*	0*	0*
lnqCPUE	-6.0	-6.1	-5.8	-6.1	-6.1	-5.4	-6.0	-6.0
lnqCR	-3.4	-3.4	-3.3	-3.4	-3.4	-1.6	-3.4	-2.3
CPUEpow	1*	1*	1*	1*	1*	1.034	1*	1*
mat50	39*	39*	39*	39*	39*	39*	39*	39*
mat95 - mat50	14*	14*	14*	14*	14*	14*	14*	14*
GalphaM1	4.4	4.3	4.2	4.4	4.4	4.4	4.3	4.4
GBetaM1	4.4	3.6	4.2	3.7	4.4	4.4	4.3	4.4
GdiffM1	0.995	0.8	1.000	0.8	1.000	0.99	1.000	1.000
GshapeM1	6.8	5.8	7.8	5.8	6.9	6.7	6.8	6.7
GrowthCVM1	0.5*	0.5*	0.5*	0.5*	0.5*	0.5*	0.53	0.5*
GalphaF1	1.5	1.6	1.5	1.5	1.5	1.5	1.6	1.5
GBetaF1	1.4	1.4	1.5	1.2	1.3	1.4	1.4	1.4
GdiffF1	0.9	0.9	1.000	0.8	0.9	0.9	0.9	0.9
GshapeF1	15.0	15.0	15.0	15.0	15.0	15.0	15.0	15.0
GrowthCVF1	0.5*	0.5*	0.5*	0.5*	0.5*	0.5*	0.96	0.5*
GalphaM2	2.3	2.4	2.3	2.4	2.3	2.3	2.1	2.2
GBetaM2	1.9	2.1	1.9	2.1	1.8	1.9	2.1	1.7

	base case	Alter treatment of growth transition period			Change model estimation assumptions			
Trial number		1	2	3	4	5	6	7
Trial name		1981-82	1994-95	1985-90	finite	CPUEpow	GCV	domed
GdiffM2	0.8	0.9	0.8	0.9	0.8	0.8	0.963	0.8
GshapeM2	15.0	15.0	15.0	15.0	15.0	15.0	15.0	15.0
GrowthCVM2	0.5*	0.5*	0.5*	0.5*	0.5*	0.5*	0.70	0.5*
GalphaF2	1.1	1.2	1.2	1.2	1.1	1.1	1.1	0.7
GBetaF2	0.6	0.3	0.1	0.4	0.7	0.6	0.6	0.7
GdiffF2	0.5	0.3	0.1	0.4	0.7	0.5	0.5	0.996
GshapeF2	0.1	0.1	0.1	0.1	0.1	0.1	0.1	0.1
GrowthCVF2	0.5*	0.5*	0.5*	0.5*	0.5*	0.5*	0.505	0.5*
vuln1	0.84	0.86	0.82	0.85	0.84	0.85	0.85	0.94
vuln2	0.41	0.41	0.31	0.39	0.44	0.41	0.40	0.65
vuln3	1.00	1.00	1.00	1.00	1.00	1.00	1.00	1.00
vuln4	0.33	0.33	0.33	0.32	0.36	0.33	0.33	0.35
varL1M	4.58	5.12	4.10	5.10	4.40	4.57	4.40	4.37
varR1M	200*	200*	200*	200*	200*	200*	200*	5.5
SelMax1M	53.4	53.8	53.1	53.9	52.5	53.4	53.4	53.0
varL 1F	8.1	7.1	10.0	7.1	7.3	8.0	8.0	8.3
varR 1F	200*	200*	200*	200*	200*	200*	200*	3.4
SelMax1F	65.3	63.1	69.8	63.0	62.7	56.0	65.0	66.0
varL 2M	6.0	5.9	5.5	6.0	5.9	6.0	5.6	6.4
varR 2M	200*	200*	200*	200*	200*	200*	200*	12.2
SelMax2M	54.4	54.3	54.5	54.4	53.8	53.9	54.4	54.7
varL 2F	8.8	9.0	9.6	8.8	8.3	8.8	8.8	9.0
varR 2F	200*	200*	200*	200*	200*	200*	200*	7.1
SelMax2F	68.0	68.4	70.0	68.0	66.7	68.0	68.1	69.2

	base case	Alter treatment of growth transition period			Change model estimation assumptions			
Trial number		1	2	3	4	5	6	7
Trial name		1981-82	1994-95	1985-90	finite	CPUEpow	GCV	domed
Bref	783.7	816.5	668.4	810.9	796.9	963.4	782.0	944.2
depletion	0.40	0.40	0.40	0.40	0.42	0.27	0.40	0.35
Bcurr	311.8	327.6	264.2	325.4	330.9	258.3	315.0	328.4
Bmsy1	603.0	467.9	439.9	518.8	#N/A	404.5	548.7	506.9
Bcurr/Bmsy1	0.52	0.70	0.60	0.63	#N/A	0.64	0.57	0.65
MSY1	338.4	248.4	226.6	240.4	#N/A	413.1	238.5	405.1
Fmult1	0.5	0.7	0.5	0.6	#N/A	1.4	0.5	1.0
Bmsy2	220.2	279.0	222.5	272.4	#N/A	764.8	249.9	567.4
Bcurr/Bmsy2	1.42	1.17	1.19	1.19	#N/A	0.34	1.26	0.58
MSY2	249.1	163.6	148.8	162.2	#N/A	360.2	140.1	267.6
Fmult2	1.2	1.0	0.9	1.0	#N/A	0.6	0.9	0.7

Table 8: Results of MPD sensitivity trials 8–14.

	base case	Change model estimation assumptions (cont.)			Treatment of NSL catch			
Trial number		8	9	10	11	12	13	14
Trial name		fixM	estmat	SelMaxF60	hiCVCnsl	scaler	halfillegal	noMR
Total function value	8556.7	8572.3	8527.0	8630.7	8531.9	8526.9	8537.9	8558.8
LFs-sdnr	1.76	2.00	1.52	1.81	1.67	1.83	1.79	1.81
LFs-MAR	0.51	0.51	0.45	0.51	0.50	0.49	0.50	0.50
LFs-LL	1136.4	1127.6	1098.4	1204.2	1112.2	1115.1	1125.4	1139.7
Tags-sdnr	1.36	1.36	1.37	1.36	1.36	1.36	1.36	1.36
Tags-MAR	0.71	0.71	0.71	0.71	0.71	0.71	0.71	0.71
Tags-LL	7392.4	7384.1	7389.8	7395.0	7392.4	7387.1	7389.5	7391.1
CPUE- sdnr	1.29	1.33	1.29	1.35	1.19	1.31	1.29	1.30
CPUE-MAR	0.83	0.84	0.87	0.67	0.77	0.88	0.85	0.78
CPUE-LL	-18.6	-16.0	-19.1	-14.2	-26.1	-17.0	-18.6	-18.5
CR-sdnr	0.35	0.37	0.36	0.35	0.35	0.34	0.34	0.35
CR-MAR	0.18	0.25	0.21	0.19	0.18	0.16	0.18	0.18
CR-LL	41.3	41.4	41.3	41.3	41.3	41.3	41.3	41.3
Catch-LL	0.9	0.9	0.8	0.9	18.0	1.0	0.9	1.0
Prior contributions	4.2	34.3	15.9	3.5	-5.8	-0.7	-0.5	4.2
lnR0	13.6	13.3	13.5	13.6	13.7	13.5	13.6	13.6
M	0.16	0.12*	0.14	0.15	0.17	0.17	0.16	0.16
InitER	0*	0*	0*	0*	0*	0*	0*	0*

	base case	Change model estimation assumptions (cont.)			Treatment of NSL catch			
Trial number		8	9	10	11	12	13	14
Trial name		fixM	estmat	SelMaxF60	hiCVCnsl	scaler	halfillegal	noMR
lnqCPUE	-6.0	-6.0	-6.0	-6.0	-6.1	-5.9	-6.0	-6.0
lnqCR	-3.4	-3.6	-3.5	-3.4	-3.5	-3.2	-3.4	-3.4
CPUEpow	1*	1*	1*	1*	1*	1*	1*	1*
mat50	39*	39*	41.4	39*	39*	39*	39*	39*
mat95 - mat50	14*	14*	80.0	14*	14*	14*	14*	14*
GalphaM1	4.4	4.4	4.4	4.4	4.4	4.4	4.4	4.4
GBetaM1	4.4	4.2	4.3	4.3	4.4	4.4	4.4	4.4
GdiffM1	0.995	0.9	0.968	0.986	1.000	1.000	1.000	1.000
GshapeM1	6.8	6.3	6.6	6.7	6.8	6.8	6.8	6.8
GrowthCVM1	0.5*	0.5*	0.5*	0.5*	0.5*	0.5*	0.5*	0.5*
GalphaF1	1.5	1.5	1.4	1.5	1.6	1.6	1.6	1.5
GBetaF1	1.4	1.3	1.3	1.2	1.4	1.5	1.4	1.4
GdiffF1	0.9	0.9	0.9	0.8	0.9	0.9	0.9	0.9
GshapeF1	15.0	15.0	15.0	15.0	15.0	15.0	15.0	15.0
GrowthCVF1	0.5*	0.5*	0.5*	0.5*	0.5*	0.5*	0.5*	0.5*
GalphaM2	2.3	2.3	2.3	2.3	2.3	2.3	2.3	2.3
GBetaM2	1.9	1.8	1.9	1.9	1.9	1.9	1.9	1.9
GdiffM2	0.8	0.8	0.8	0.8	0.8	0.8	0.8	0.8
GshapeM2	15.0	15.0	15.0	15.0	15.0	15.0	15.0	15.0
GrowthCVM2	0.5*	0.5*	0.5*	0.5*	0.5*	0.5*	0.5*	0.5*
GalphaF2	1.1	0.8	0.9	1.3	1.2	1.2	1.1	1.0
GBetaF2	0.6	0.6	0.8	0.0	0.4	0.3	0.5	0.6
GdiffF2	0.5	0.7	0.9	0.001	0.3	0.3	0.4	0.6
GshapeF2	0.1	0.1	0.1	0.1	0.1	0.1	0.1	0.1
GrowthCVF2	0.5*	0.5*	0.5*	0.5*	0.5*	0.5*	0.5*	0.5*
vuln1	0.84	0.87	0.84	0.85	0.85	0.83	0.84	0.84
vuln2	0.41	0.54	0.24	0.13	0.36	0.37	0.39	0.43
vuln3	1.00	1.00	1.00	0.34	1.00	1.00	1.00	1.00
vuln4	0.33	0.33	0.33	0.11	0.33	0.32	0.33	0.32
varL1M	4.58	4.63	4.60	4.62	4.59	4.62	4.61	4.61
varR1M	200*	200*	200*	200*	200*	200*	200*	200*
SelMax1M	53.4	53.4	53.4	53.6	53.3	53.0	53.3	53.5
varL 1F	8.1	8.6	8.3	6.9	7.6	7.9	7.9	8.2
varR 1F	200*	200*	200*	200*	200*	200*	200*	200*
SelMax1F	65.3	66.3	65.9	60*	64.1	64.3	64.7	65.6
varL 2M	6.0	6.0	6.0	5.9	6.0	6.1	6.0	6.0

	base case	Change model estimation assumptions (cont.)			Treatment of NSL catch			
Trial number		8	9	10	11	12	13	14
Trial name		fixM	estmat	SelMaxF60	hiCVCnsl	scaler	halfillegal	noMR
varR 2M	200*	200*	200*	200*	200*	200*	200*	200*
SelMax2M	54.4	54.2	54.3	54.1	54.5	54.3	54.4	54.4
varL 2F	8.8	8.9	8.7	6.4	9.0	8.9	8.9	8.8
varR 2F	200*	200*	200*	200*	200*	200*	200*	200*
SelMax2F	68.0	68.8	68.1	60*	68.2	67.8	68.1	68.1
Bref	783.7	839.6	797.2	829.3	823.3	643.8	742.1	769.0
depletion	0.40	0.39	0.39	0.38	0.42	0.42	0.40	0.40
Bcurr	311.8	326.2	309.1	311.7	341.9	272.3	296.4	305.3
Bmsy1	603.0	718.3	768.5	552.7	546.6	367.3	600.1	641.9
Bcurr/Bmsy1	0.52	0.45	0.40	0.56	0.63	0.74	0.49	0.48
MSY1	338.4	193.3	215.5	219.3	248.6	174.6	327.5	367.6
Fmult1	0.5	0.3	0.3	0.5	0.6	0.5	0.5	0.5
Bmsy2	220.2	254.5	240.1	227.7	260.8	185.5	247.5	234.1
Bcurr/Bmsy2	1.42	1.28	1.29	1.37	1.31	1.47	1.20	1.30
MSY2	249.1	101.8	125.3	147.0	160.7	103.8	233.5	266.5
Fmult2	1.2	0.6	0.8	1.1	1.1	0.8	1.1	1.2

Table 9: Results of MPD sensitivity trials 15–23.

	base case	Alter model initialisation assumptions						Effect of data sets		
Trial number		15	16	17	18	19	20	21	22	23
Trial name		start63.1	start63.4	start63.7	start73.1	start73.4	start73.7	noLF	notags	noCPUE
Total function value	8556.7	8574.8	8553.6	8544.1	8589.5	8539.2	8519.1	7306.6	1112.6	8508.8
LFs-sdnr	1.76	1.78	1.94	2.03	1.83	1.88	1.97	114186.00	3.74	2.26
LFs-MAR	0.51	0.51	0.51	0.52	0.50	0.51	0.51	2.53	0.52	0.51
LFs-LL	1136.4	1136.3	1127.3	1125.4	1150.6	1133.0	1129.0	44536.8	1118.8	1119.6
Tags-sdnr	1.36	1.36	1.36	1.36	1.38	1.36	1.36	1.34	1.77	1.34
Tags-MAR	0.71	0.71	0.71	0.71	0.71	0.71	0.71	0.69	0.76	0.71
Tags-LL	7392.4	7392.5	7386.6	7384.2	7404.1	7384.8	7381.8	7353.0	7724.3	7373.9
CPUE- sdnr	1.29	1.30	1.28	1.28	1.51	1.44	1.40	0.66	1.17	5.26
CPUE-MAR	0.83	0.84	0.80	0.77	0.86	0.81	0.79	0.44	0.88	1.46
CPUE-LL	-18.6	-17.9	-19.7	-19.7	-1.1	-6.6	-10.3	-54.5	-27.4	835.8
CR-sdnr	0.35	0.53	0.68	0.74	1.42	0.11	0.72	0.36	0.33	0.82
CR-MAR	0.18	0.41	0.37	0.36	0.02	0.06	0.05	0.13	0.22	0.61

	base case	Alter model initialisation assumptions						Effect of data sets		
Trial number		15	16	17	18	19	20	21	22	23
Trial name		start63.1	start63.4	start63.7	start73.1	start73.4	start73.7	noLF	notags	noCPUE
CR-LL	41.3	42.2	43.2	43.7	9.4	5.3	6.3	41.4	41.2	44.3
Catch-LL	0.9	0.9	0.9	0.9	1.0	0.9	0.8	0.0	0.9	0.3
Prior contributions	4.2	20.7	15.3	9.6	34.8	27.2	17.7	-33.3	-20.9	-29.3
lnR0	13.6	13.6	13.5	13.5	13.5	13.4	13.5	14.7	13.9	13.7
M	0.16	0.16	0.13	0.12	0.17	0.13	0.12	0.35	0.17	0.15
InitER	0*	0.1*	0.4*	0.7*	0.1*	0.4*	0.7*	0*	0*	0*
lnqCPUE	-6.0	-6.0	-6.0	-6.0	-6.1	-6.1	-6.1	-5.9	-5.8	-6*
lnqCR	-3.4	-3.5	-2.7	-2.2	-3.0	-3.0	-3.0	-2.7	-3.1	-4.4
CPUEpow	1*	1*	1*	1*	1*	1*	1*	1*	1*	1*
mat50	39*	39*	39*	39*	39*	39*	39*	39*	39*	39*
mat95 - mat50	14*	14*	14*	14*	14*	14*	14*	14*	14*	14*
GalphaM1	4.4	4.4	4.4	4.4	4.4	4.4	4.4	4.4	3.4	4.4
GBetaM1	4.4	4.1	4.4	4.4	1.5	4.0	4.4	4.2	0.0	4.4
GdiffM1	0.995	0.9	0.993	1.000	0.3	0.9	1.000	0.97	0.001	1.000
GshapeM1	6.8	6.4	6.7	6.7	3.0	6.1	6.8	6.6	5.1	6.8
GrowthCVM1	0.5*	0.5*	0.5*	0.5*	0.5*	0.5*	0.5*	0.5*	0.5*	0.5*
GalphaF1	1.5	1.5	1.5	1.5	1.5	1.5	1.5	1.7	1.4	1.7
GBetaF1	1.4	1.3	1.4	1.4	1.3	1.3	1.3	1.5	0.0	1.6
GdiffF1	0.9	0.9	0.9	0.9	0.9	0.9	0.9	0.9	0.001	0.9
GshapeF1	15.0	15.0	15.0	15.0	15.0	15.0	15.0	15.0	4.3	15.0
GrowthCVF1	0.5*	0.5*	0.5*	0.5*	0.5*	0.5*	0.5*	0.5*	0.5*	0.5*
GalphaM2	2.3	2.3	2.3	2.3	2.3	2.3	2.3	1.9	2.9	2.2
GBetaM2	1.9	1.9	1.9	1.9	1.9	1.8	1.8	0.7	2.9	1.6
GdiffM2	0.8	0.8	0.8	0.8	0.8	0.8	0.8	0.4	1.000	0.7
GshapeM2	15.0	15.0	15.0	15.0	15.0	15.0	15.0	15.0	15.0	15.0
GrowthCVM2	0.5*	0.5*	0.5*	0.5*	0.5*	0.5*	0.5*	0.5*	0.5*	0.5*
GalphaF2	1.1	1.1	0.9	0.8	1.2	0.9	0.8	0.5	1.2	1.0
GBetaF2	0.6	0.6	0.6	0.6	0.5	0.5	0.6	0.3	0.6	0.1
GdiffF2	0.5	0.5	0.6	0.7	0.4	0.6	0.7	0.6	0.5	0.1
GshapeF2	0.1	0.1	0.1	0.1	0.1	0.1	0.1	0.1	0.1	0.1
GrowthCVF2	0.5*	0.5*	0.5*	0.5*	0.5*	0.5*	0.5*	0.5*	0.5*	0.5*
vuln1	0.84	0.85	0.89	0.89	0.86	0.91	0.92	0.77	0.81	1.00
vuln2	0.41	0.42	0.52	0.56	0.39	0.51	0.56	1.00	0.37	0.50
vuln3	1.00	1.00	1.00	1.00	1.00	1.00	1.00	1.00	1.00	1.00
vuln4	0.33	0.33	0.34	0.34	0.34	0.35	0.35	1.00	0.31	0.38
varL1M	4.58	4.58	4.62	4.63	4.52	4.60	4.62	19.39	4.63	4.66

	base case	Alter model initialisation assumptions						Effect of data sets		
Trial number		15	16	17	18	19	20	21	22	23
Trial name		start63.1	start63.4	start63.7	start73.1	start73.4	start73.7	noLF	notags	noCPUE
varR1M	200*	200*	200*	200*	200*	200*	200*	200*	200*	200*
SelMax1M	53.4	53.4	53.4	53.4	53.3	53.3	53.3	80.0	53.4	53.1
varL 1F	8.1	8.1	8.5	8.6	7.9	8.5	8.7	8.4	8.4	7.9
varR 1F	200*	200*	200*	200*	200*	200*	200*	200*	200*	200*
SelMax1F	65.3	65.4	66.2	66.3	64.9	66.1	66.5	80.0	66.1	64.8
varL 2M	6.0	6.0	6.1	6.1	5.9	6.0	6.1	1.3	5.1	6.1
varR 2M	200*	200*	200*	200*	200*	200*	200*	200*	200*	200*
SelMax2M	54.4	54.4	54.3	54.3	54.2	54.1	54.1	55.0	53.5	54.2
varL 2F	8.8	8.8	8.9	9.0	8.7	8.9	9.0	46.0	9.4	9.8
varR 2F	200*	200*	200*	200*	200*	200*	200*	200*	200*	200*
SelMax2F	68.0	68.1	68.7	68.9	67.6	68.4	68.8	47.1	69.9	70.3
Bref	783.7	820.8	602.9	519.9	1330.4	931.3	754.5	954.0	660.3	3155.2
depletion	0.40	0.39	0.54	0.63	0.25	0.38	0.47	0.30	0.40	0.08
Bcurr	311.8	316.7	326.1	329.1	338.1	352.9	351.9	282.6	260.9	242.9
Bmsy1	603.0	582.1	1026.4	1101.3	288.9	761.2	1136.2	359.2	295.9	951.6
Bcurr/Bmsy1	0.52	0.54	0.32	0.30	1.17	0.46	0.31	0.79	0.88	0.26
MSY1	338.4	321.4	347.3	374.5	270.0	309.1	355.4	738.2	349.1	416.2
Fmult1	0.5	0.5	0.3	0.3	1.0	0.4	0.3	2.5	1.0	0.3
Bmsy2	220.2	213.0	281.4	325.0	163.8	253.1	300.9	220.2	347.9	349.3
Bcurr/Bmsy2	1.42	1.49	1.16	1.01	2.06	1.39	1.17	1.28	0.75	0.70
MSY2	249.1	237.3	238.3	246.9	208.0	216.9	236.5	483.0	341.3	281.8
Fmult2	1.2	1.2	0.9	0.8	1.5	1.0	0.9	2.5	0.8	0.7

Table 10: Summary statistics for major parameters from the CRA 3 base case McMC simulations.

Quantity	Mean	Median	5th	95th
function value *f*	8741.5	8742.6	8717.5	8762.4
lnR0	13.551	13.550	13.425	13.680
M	0.175	0.174	0.161	0.191
lnqCPUE	-5.536	-5.525	-5.664	-5.439
lnqCR	-2.699	-2.692	-2.983	-2.436
GalphaM1	4.472	4.465	4.323	4.633
GalphaM2	2.456	2.457	2.374	2.536
GalphaF1	1.508	1.505	1.389	1.632
GalphaF2	1.196	1.194	1.081	1.318
GdiffM1	0.830	0.876	0.510	0.989
GdiffM2	0.962	0.966	0.913	0.996
GdiffF1	0.865	0.871	0.740	0.972
GdiffF2	0.384	0.372	0.079	0.745
GshapeM1	5.383	5.574	3.187	6.850
GshapeM2	14.999	14.999	14.999	15.000
GshapeF1	14.999	14.999	14.998	15.000
GshapeF2	0.102	0.102	0.100	0.106
vuln[1]	0.636	0.630	0.595	0.693
vuln[2]	0.292	0.285	0.192	0.413
vuln[3]	0.999	0.999	0.999	1.000
vuln[4]	0.254	0.252	0.227	0.286
varLM1	6.300	6.154	5.139	8.018
varLM2	6.363	6.359	5.885	6.852
varLF1	9.477	9.389	8.115	11.111
varLF2	9.401	9.383	8.716	10.166
SelMaxM1	57.145	56.919	55.277	59.777
SelMaxM2	55.837	55.852	55.010	56.624
SelMaxF1	69.225	69.120	66.376	72.405
SelMaxF2	69.990	69.946	68.520	71.552
F2007SLAW	0.731	0.733	0.600	0.852
F2007NSLAW	0.160	0.162	0.134	0.184
F2007SLSS	0.748	0.740	0.624	0.898
F2007NSLSS	0.102	0.102	0.089	0.116

Table 11: Assessment indicators from the projections with 2007 catch levels and TACC. *USL* is the exploitation rate that produces the size-limited catch. All biomass values are in tonnes and represent the beginning of season AW vulnerable biomass. "Value" is the median for all but the last group of indicators, where the value is the percentage of runs where the proposition was true. Also shown are 5th and 95th quantiles.

	Indicator	Value	5%	95%
Biomass	*Bmin*	149.1	134.4	172.2
	B2008	167.1	135.1	218.7
	B2012	123.7	64.9	255.6
	Bmsy	330.4	301.2	378.1
CPUE	*CPUEcurr*	0.662	0.547	0.835
	CPUE2012	0.492	0.260	0.989
	CPUEmsy	1.314	1.178	1.476
yield	*MSY*	300.4	291.2	310.2
biomass ratios	*B2008/Bmin*	1.114	0.936	1.400
	B2008/Bmsy	0.505	0.406	0.643
	B2012/B2008	0.746	0.424	1.347
	B2012/Bmin	0.831	0.445	1.662
	B2012/Bmsy	0.372	0.195	0.759
fishing mortality	*USL2007*	0.550	0.461	0.621
	USL2012	0.811	0.392	1.546
	USL2012/USL2007	1.478	0.733	2.761
	Fmult	0.727		
probabilities	P(*2008>Bmin*)	82.5%		
	P*(B2008>Bmsy*)	0.0%		
	P*(B2012>B2008*)	24.5%		
	P(*B2012>Bmin*)	36.5%		
	P(*B2012>Bmsy*)	0.5%		
	P(*CPUE2012*>0.75)	19.0%		
	P(*USL2012>USL2007*)	78.9%		

Table 12: Results of five-year projections with alternative SL catch levels.

SL catch (t)	206.0	185.4	164.8	144.2	123.6	82.4	41.2	0.01
% of current catch	100%	90%	80%	70%	60%	40%	20%	0%
B2012	123.7	160.9	195.3	229.0	262.0	328.6	396.6	463.6
B2012/Bmin	0.831	1.073	1.307	1.532	1.754	2.199	2.645	3.090
B2012/B2008	0.746	0.948	1.151	1.346	1.548	1.942	2.340	2.740
B2012/Bmsy	0.372	0.481	0.586	0.688	0.788	0.989	1.191	1.394
CPUE2012	0.492	0.639	0.775	0.910	1.041	1.303	1.566	1.832
P(*B2012>Bmin*)	36.5%	57.0%	77.4%	92.4%	98.2%	100.0%	100.0%	100.0%
P(*B2012>B2008*)	24.5%	44.4%	67.6%	88.7%	97.7%	100.0%	100.0%	100.0%
P(*B2012>Bmsy*)	0.5%	1.4%	4.0%	9.0%	18.5%	47.8%	83.6%	98.3%
P(*CPUE2012>0.75*)	19.0%	34.6%	53.7%	73.5%	89.1%	99.1%	100.0%	100.0%

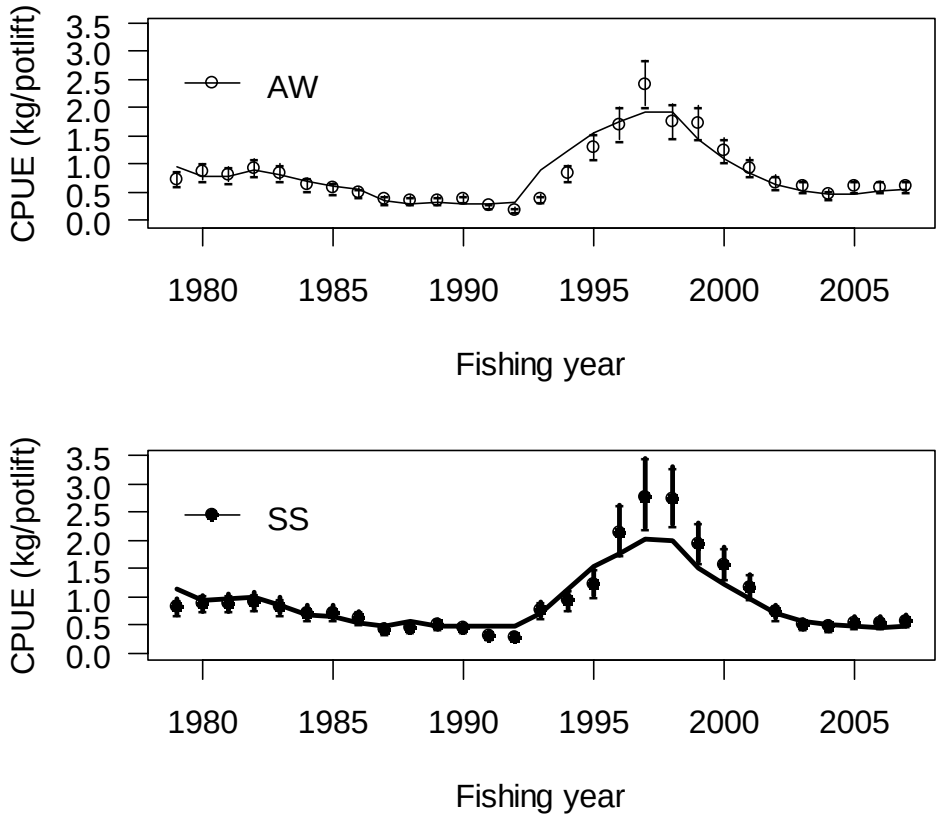

Figure 1: Observed (circles) and predicted (lines) CPUE for AW (upper) and SS from the base case MPD.

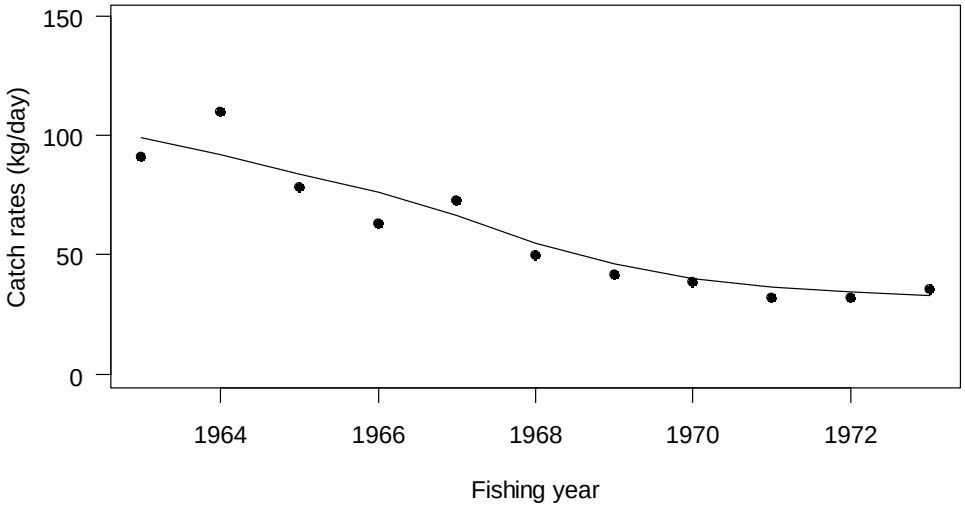

Figure 2: Observed (circles) and predicted (lines) CR from the base case MPD.

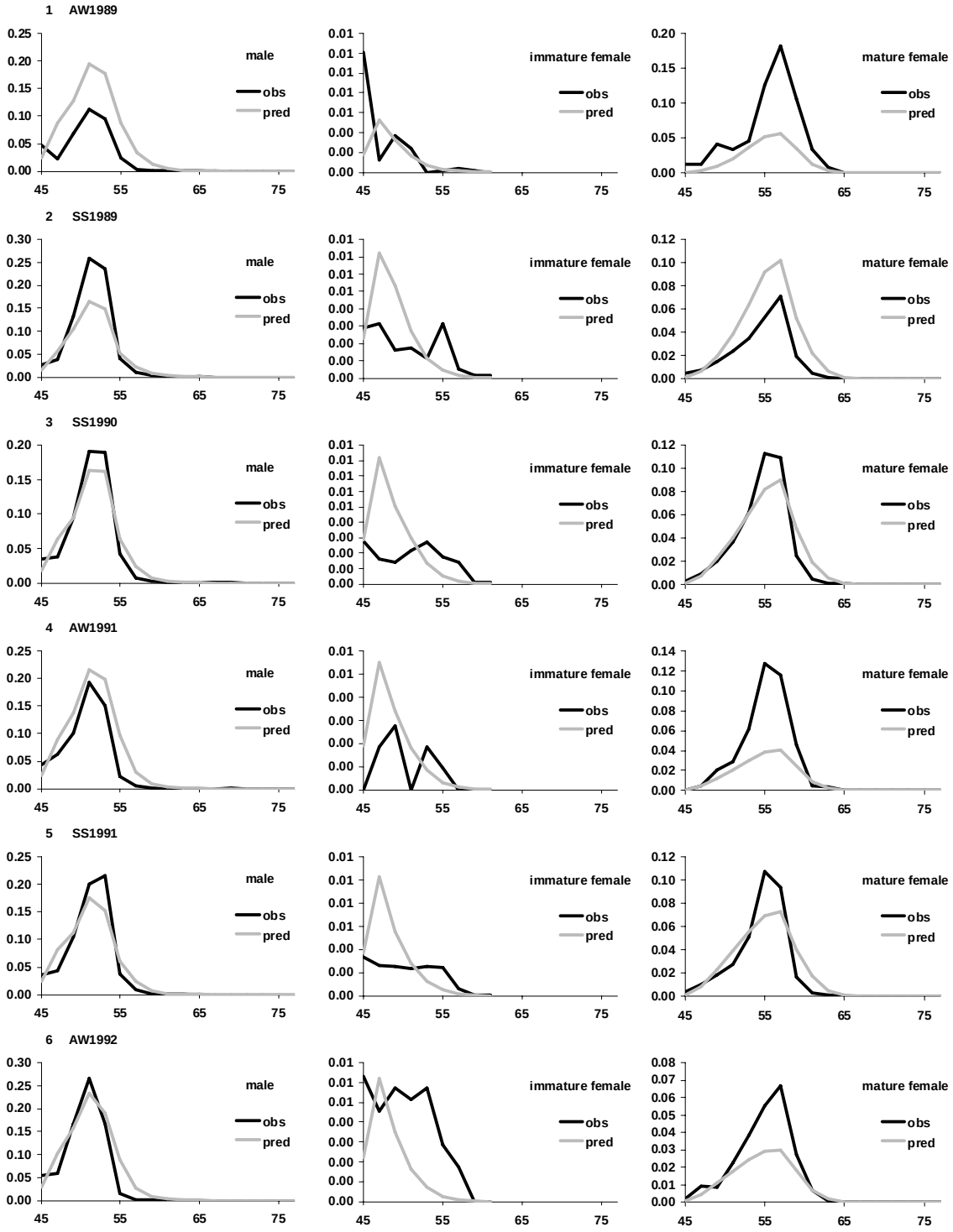

Figure 3: Observed (black) and predicted (grey) length frequencies for males (left), immature females (centre) and mature females (right) for each of the samples indicated in the left-hand corner.

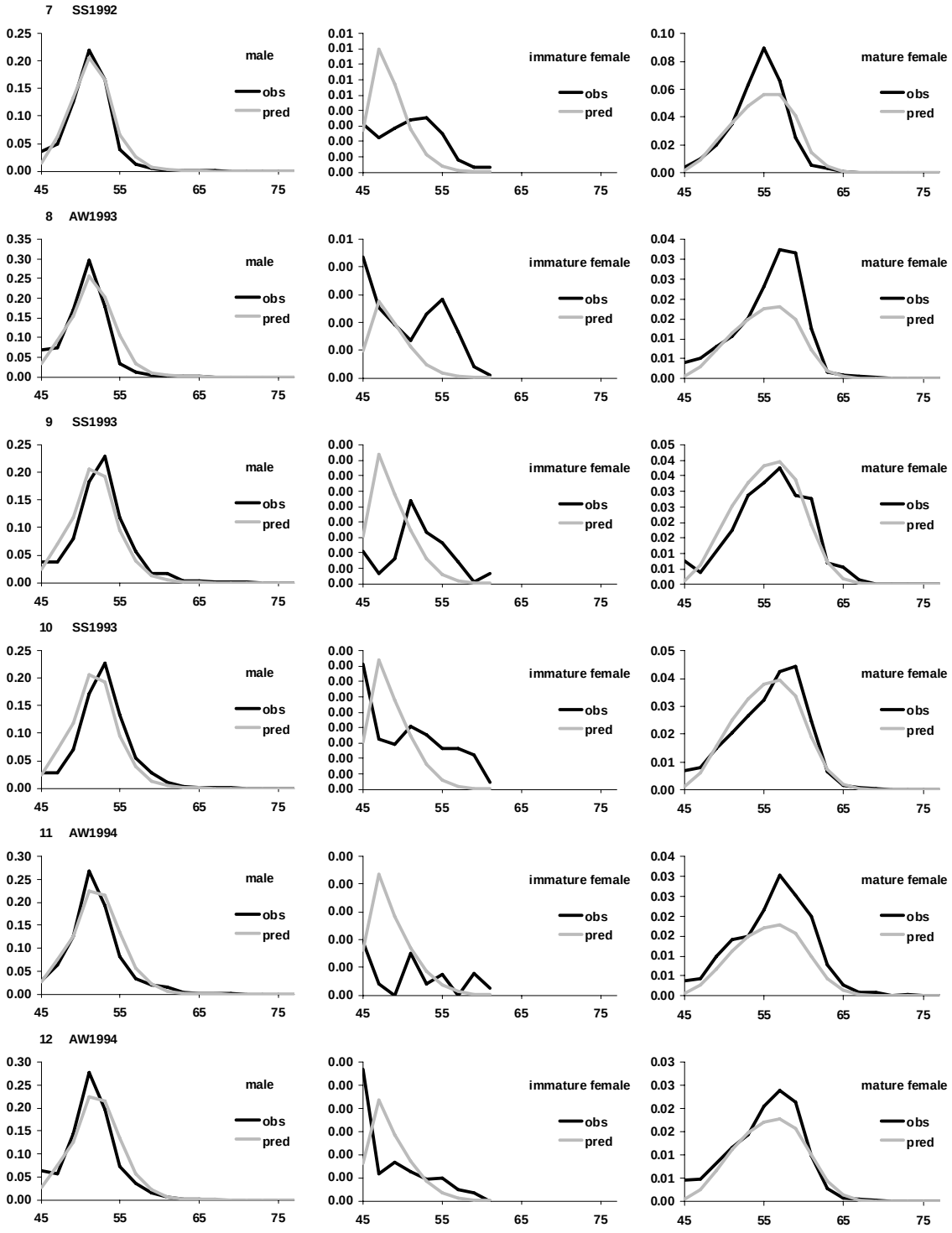

Figure 3 continued.

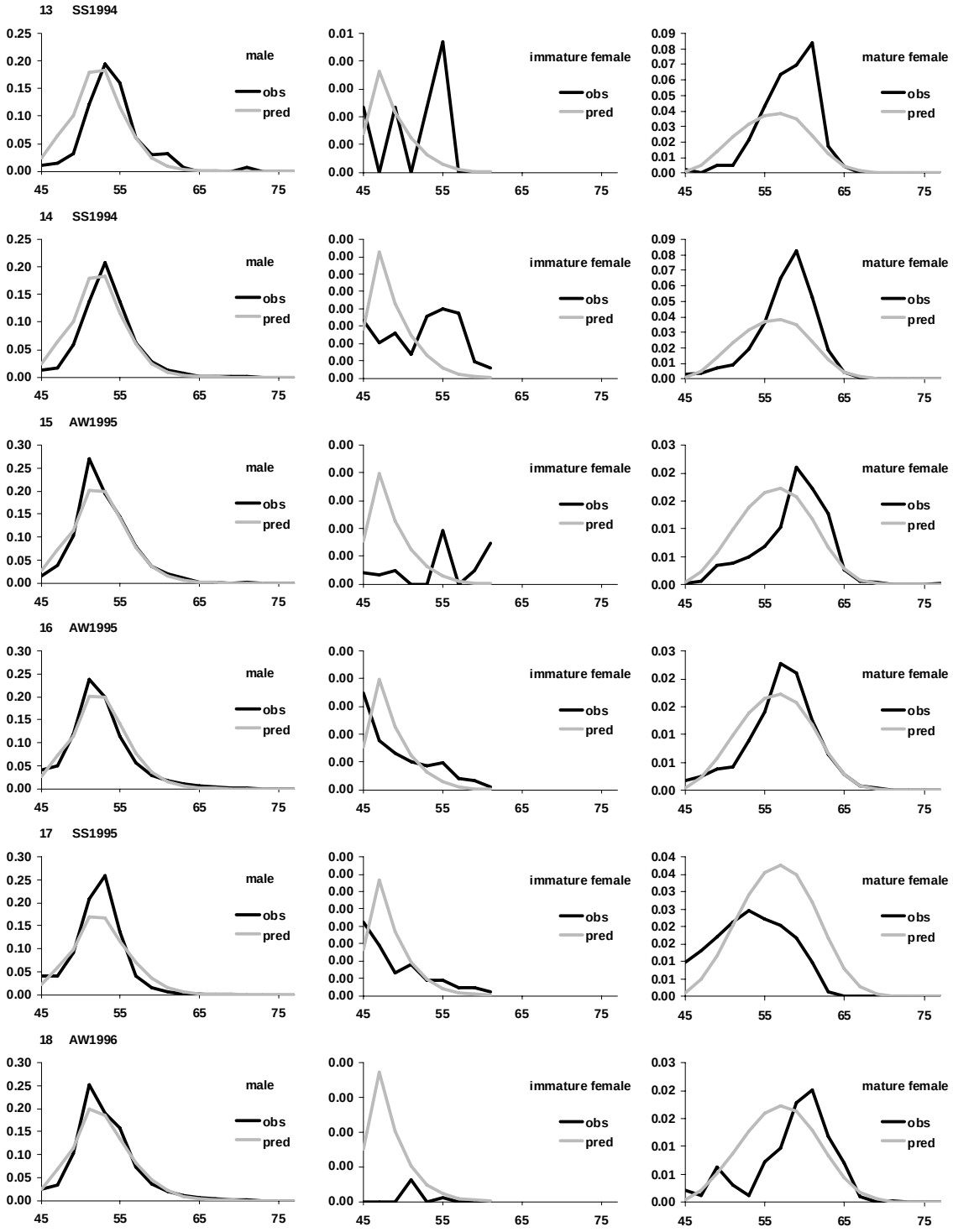

Figure 3 continued.

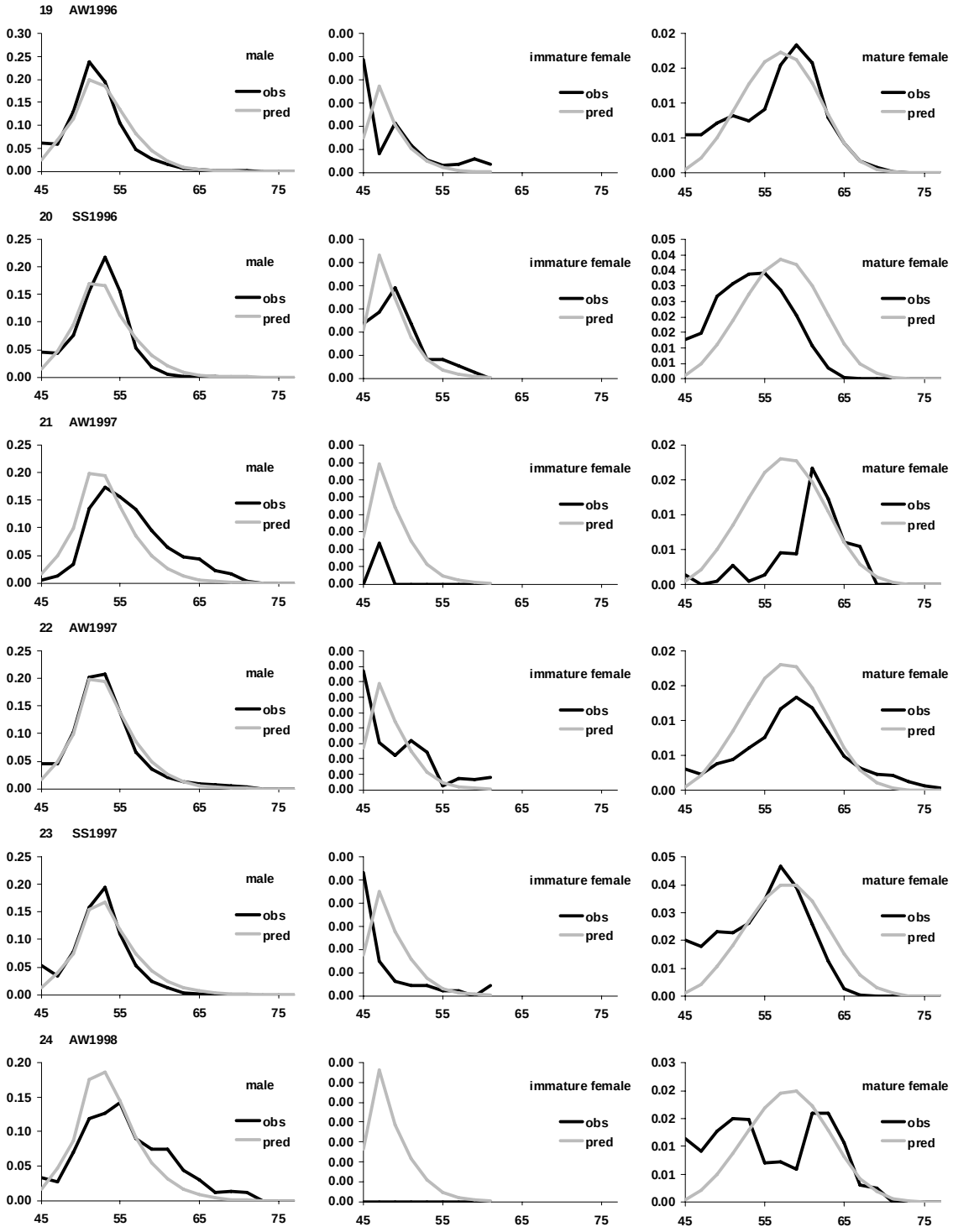

Figure 3 continued.

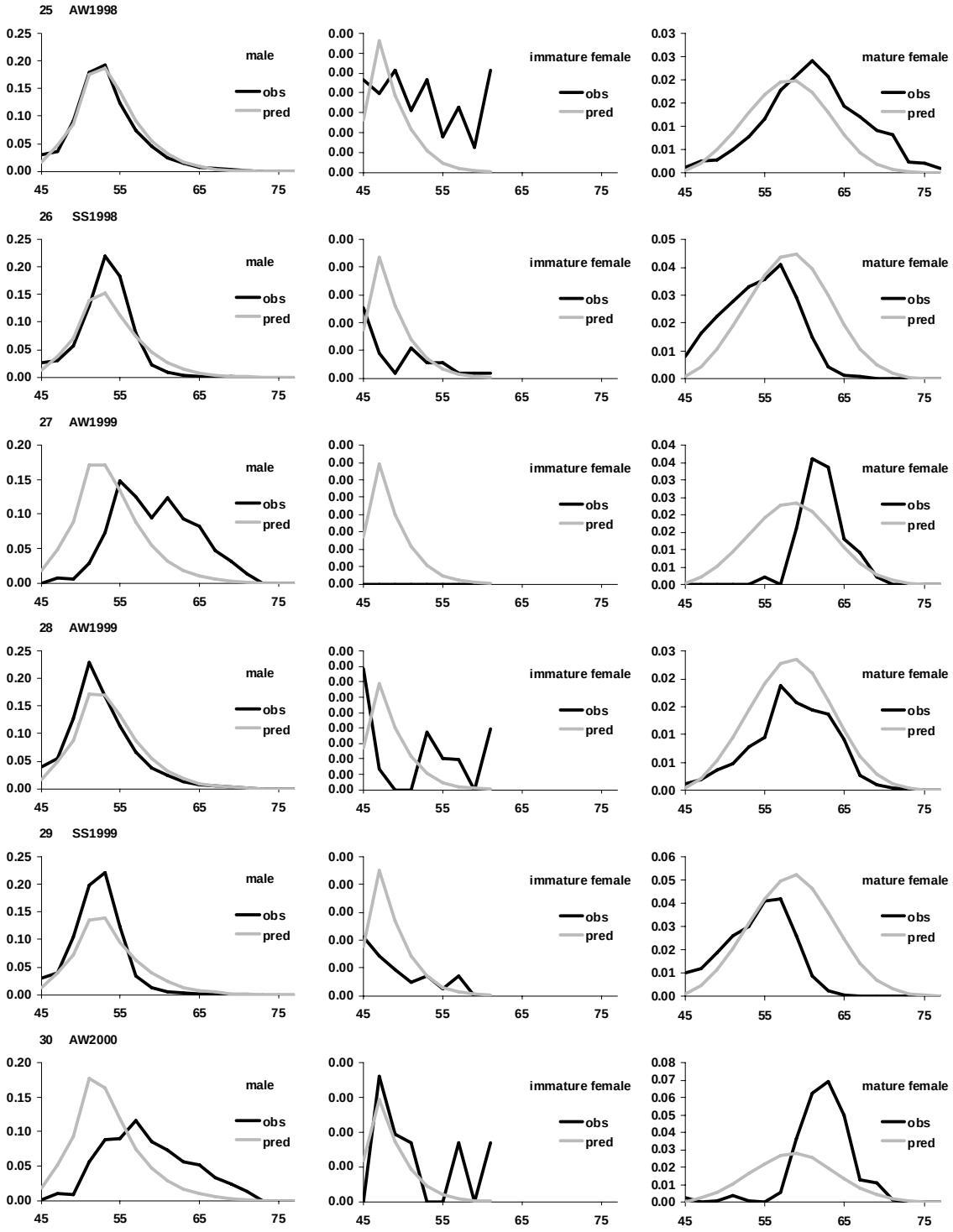

Figure 3 continued.

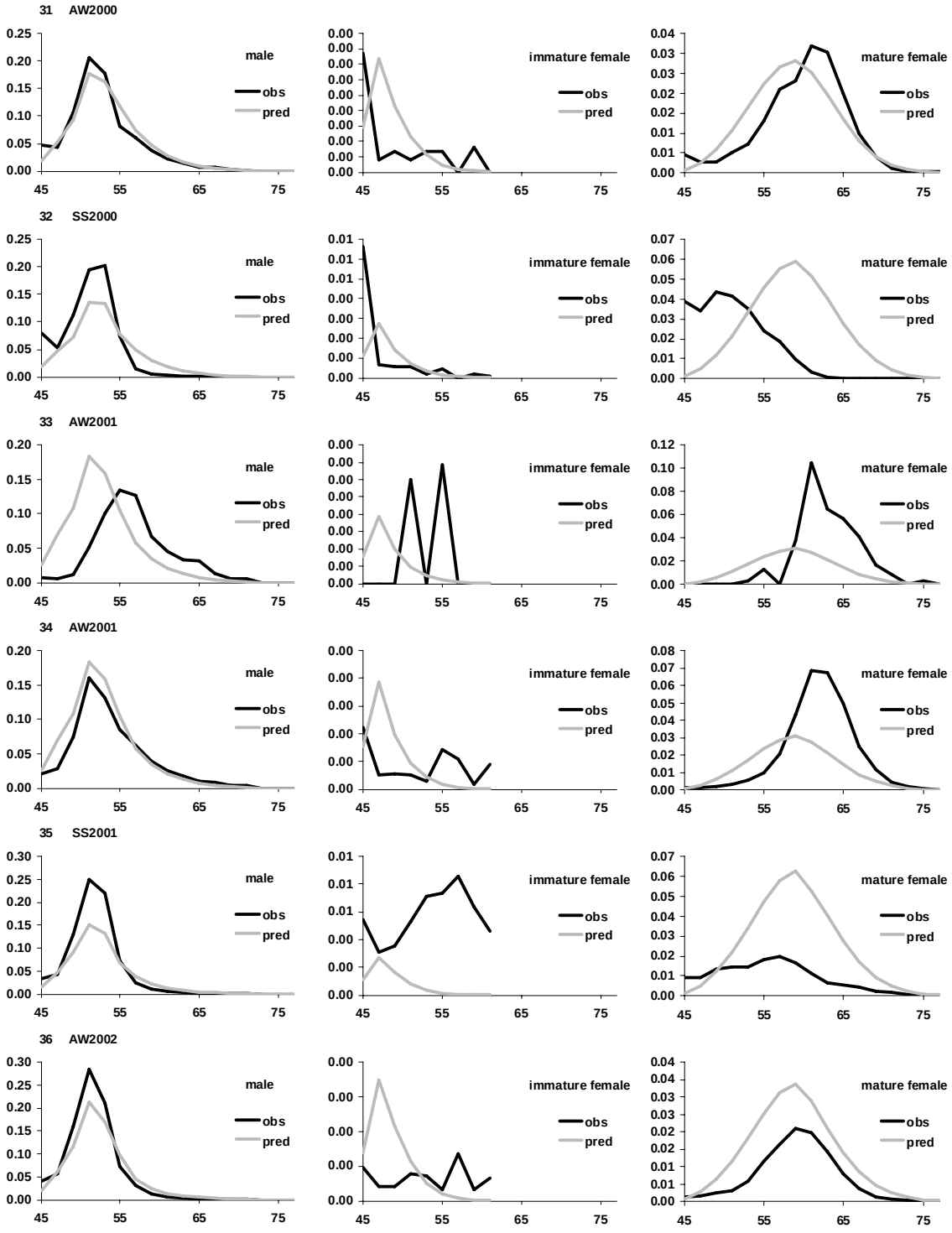

Figure 3 continued.

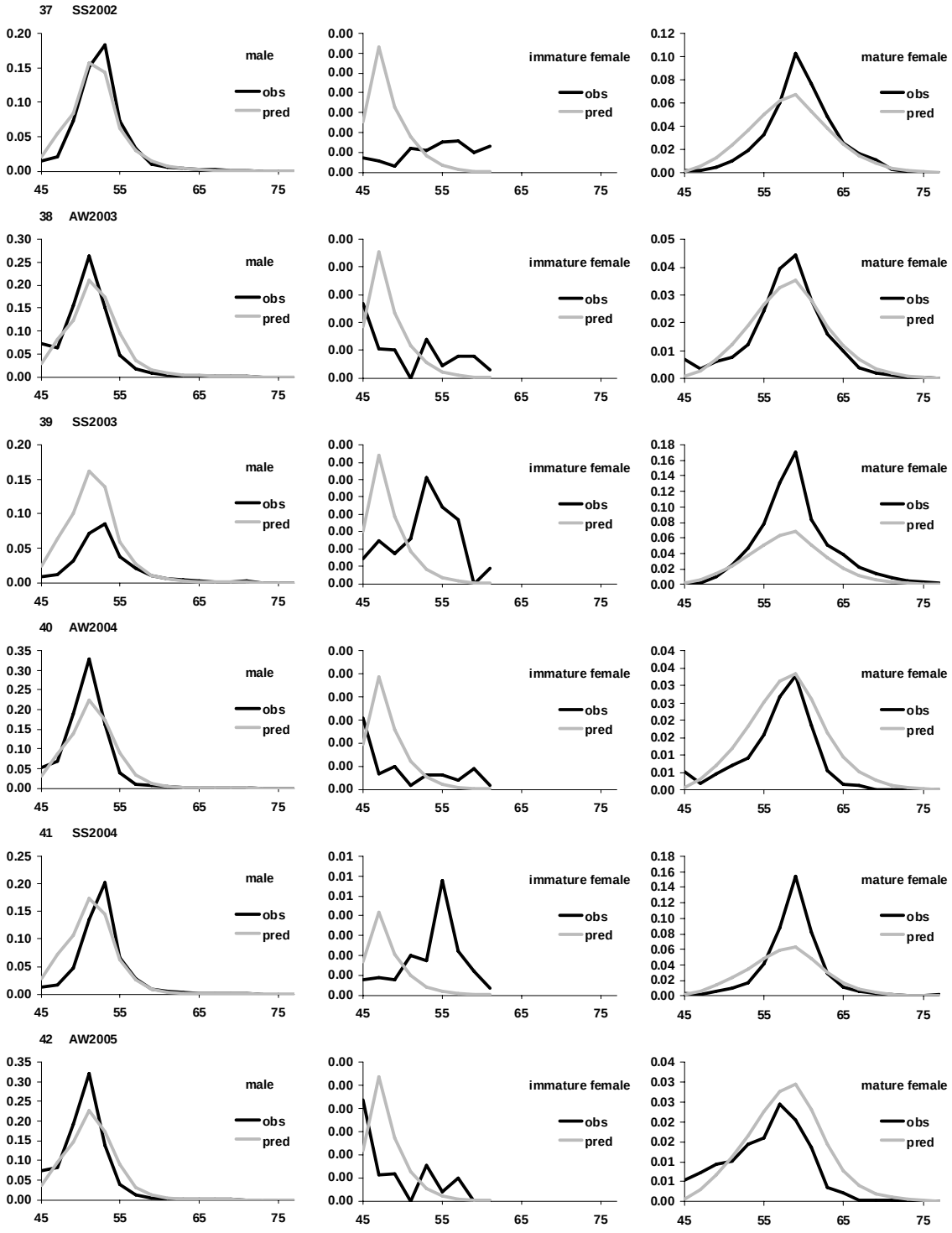

Figure 3 continued.

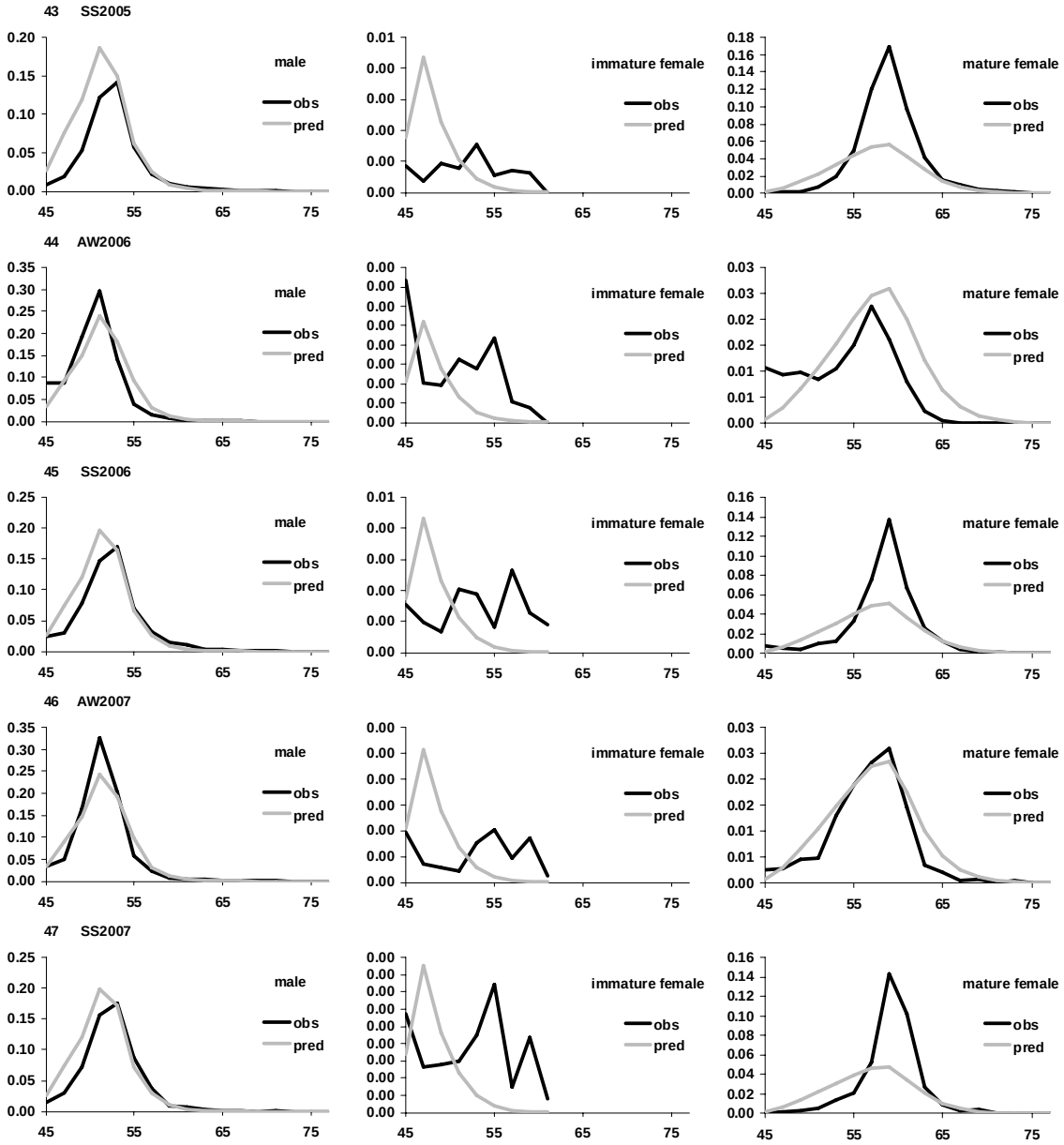

Figure 3 concluded.

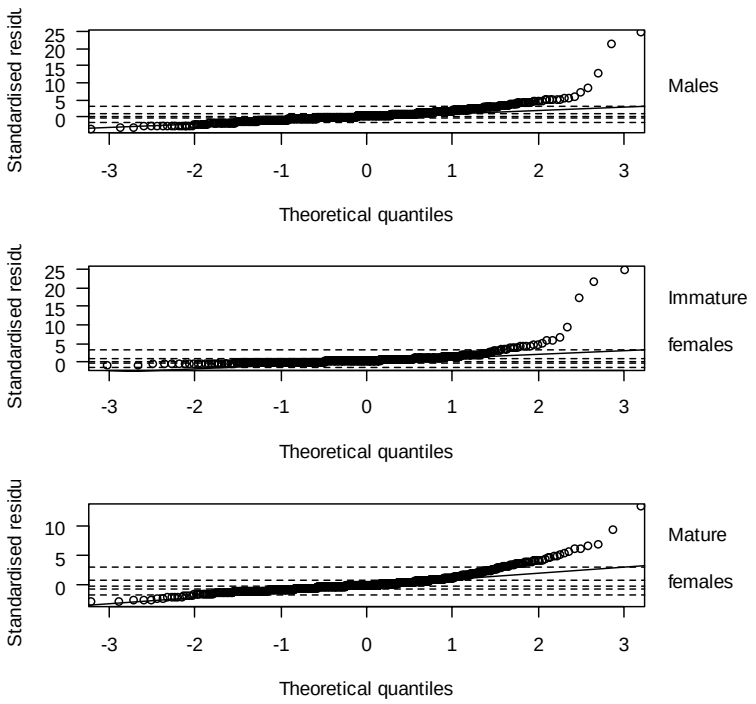

Figure 4: Q-Q plots for length frequency residuals, by sex from the CRA 3 base case MPD. Horizontal lines are 5, 25, 50, 75 and 95 percent of residuals.

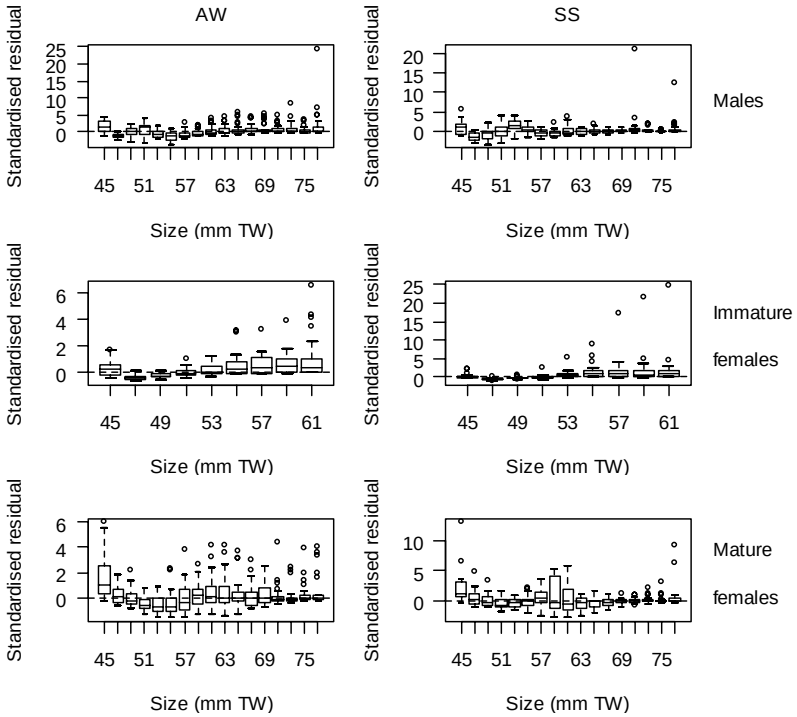

Figure 5: Box plots of standardised residuals for each size and sex class.

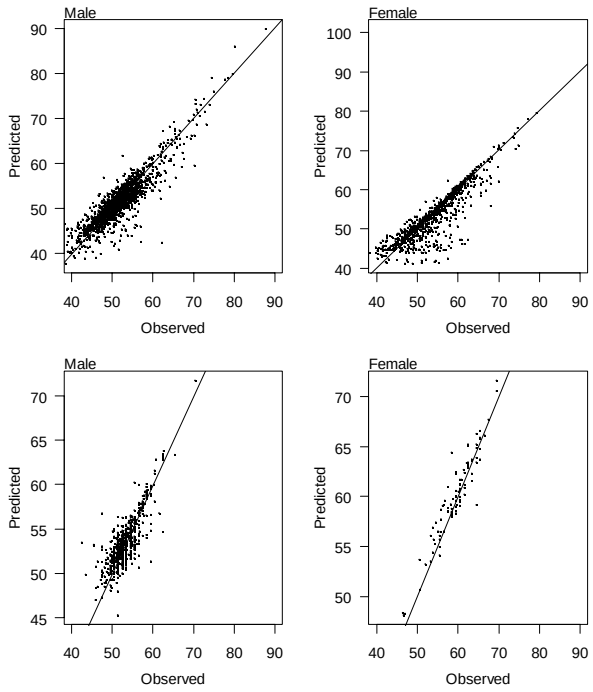

Figure 6: Predicted vs observed tag-recapture increments from males (left) and females from the earlier (upper) and later datasets in the CRA 3 base case MPD.

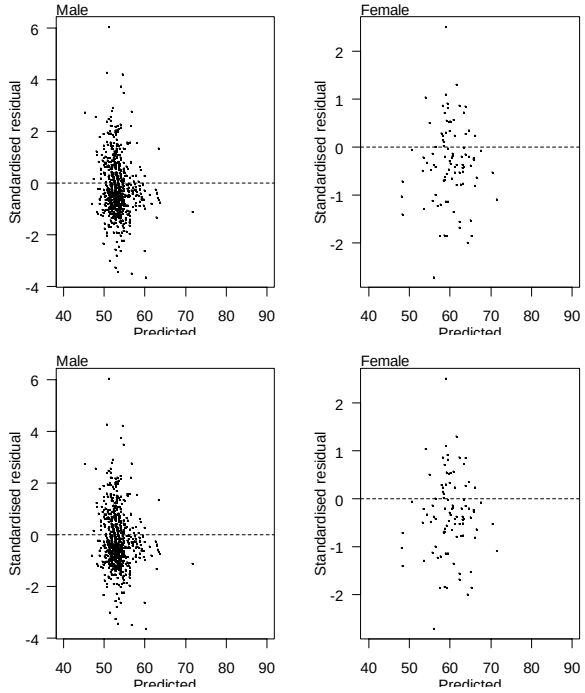

Figure 7: Normalised residuals for males (left) and females from the earlier (upper) and later datasets in the CRA 3 base case MPD.

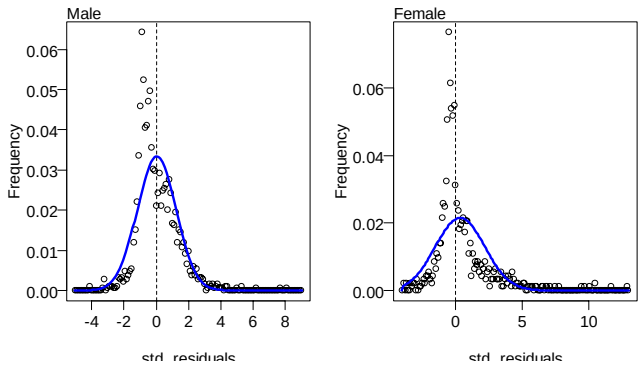

Figure 8: Actual and predicted distributions of normalised residuals from the first tag-recapture data set in the CRA 3 base case MPD.

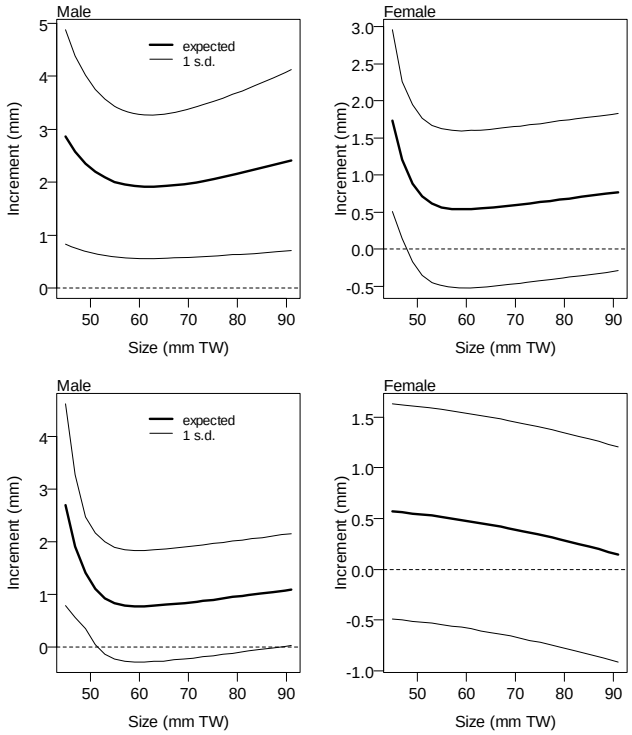

Figure 9: Predicted increments-at-length for males (left) and females from the fits to the earlier (upper) and later datasets in the CRA 3 base case MPD.

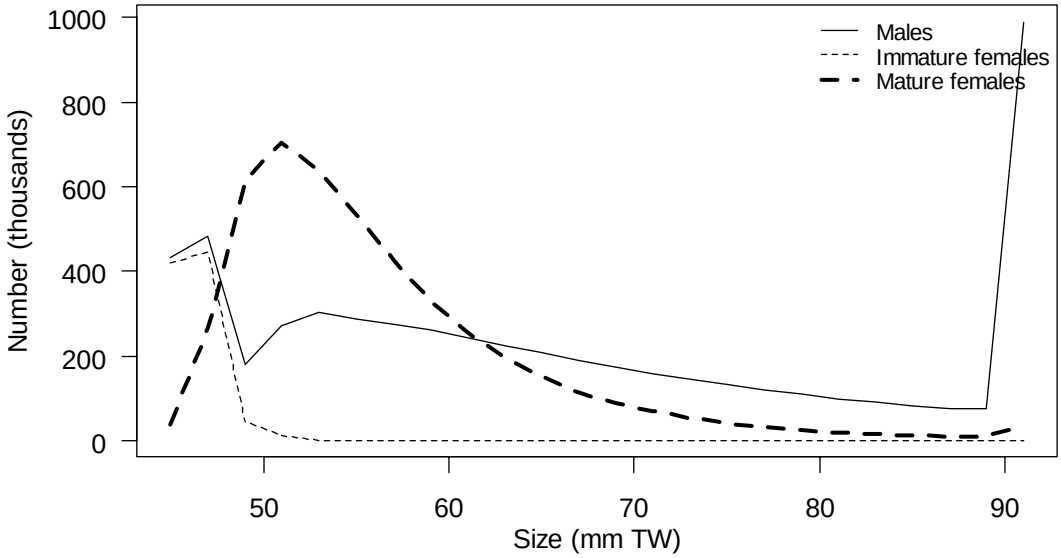

Figure 10: Initial equilibrium size frequencies by sex from the CRA 3 base case MPD.

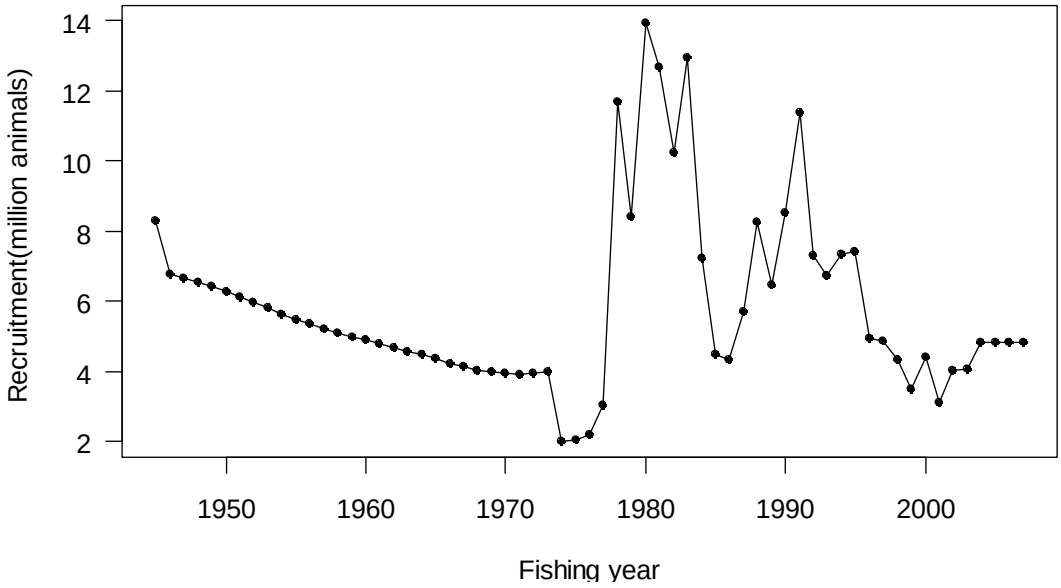

Figure 11: Annual recruitment from the CRA 3 base case MPD. Note the truncated axis.

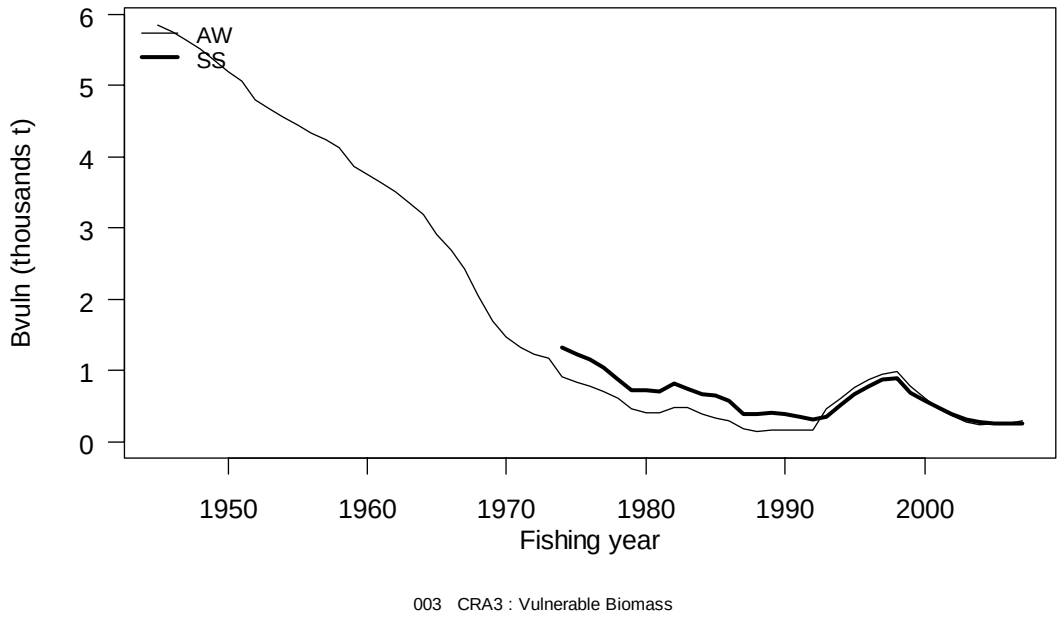

Figure 12: Vulnerable biomass trajectories, by season, from the CRA 3 MPD. There is no SS value before 1979 because the model was using a one-year time step before 1979. Vulnerable biomass is shown based on 2007 selectivities, vulnerabilities and MLS.

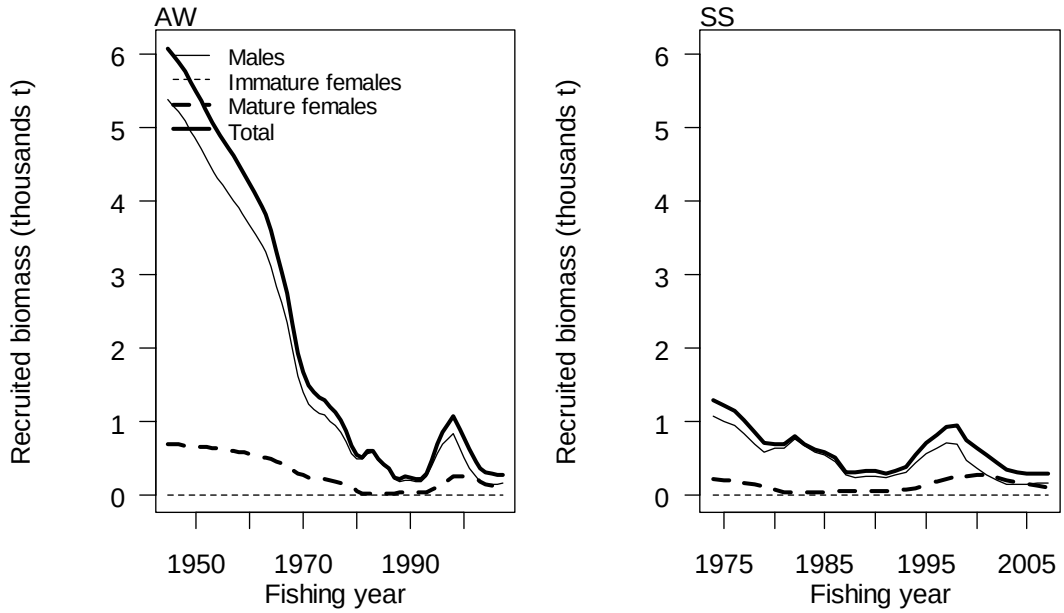

Figure 13: Recruited biomass trajectories by sex from the CRA 3 base case MPD.

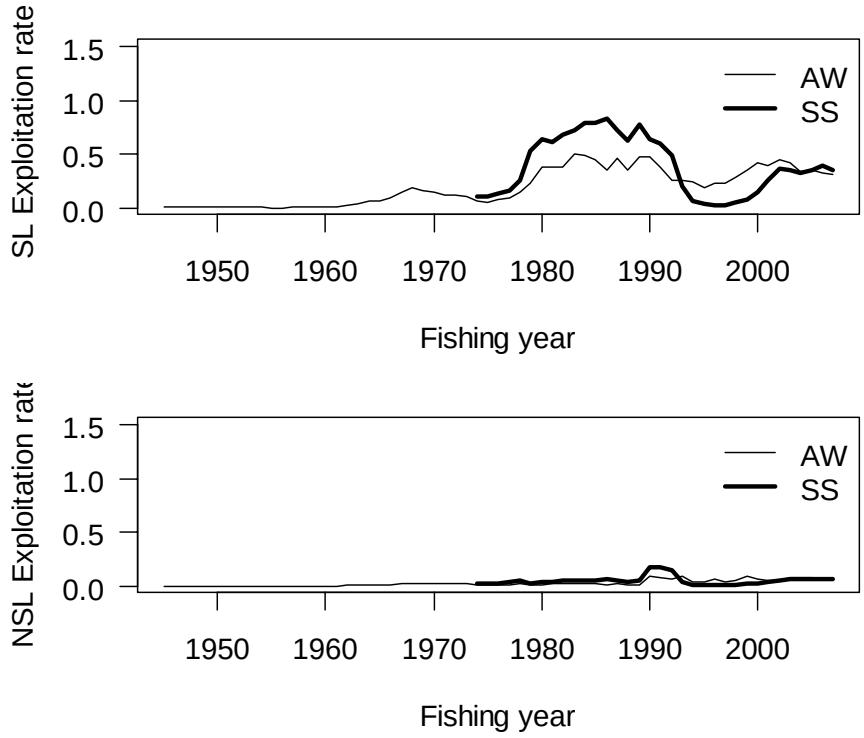

Figure 14: Trajectories for SL (upper) and NSL exploitation rate from the CRA 3 base case MPD.

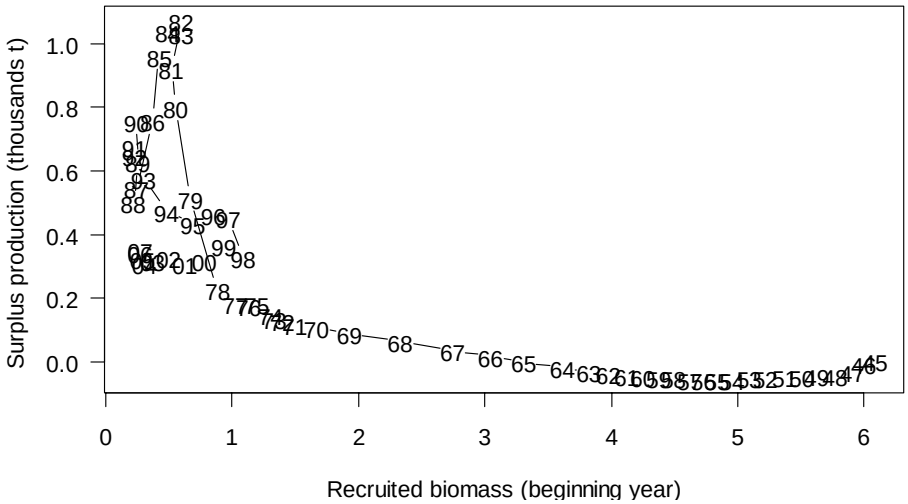

Figure 15: Estimated surplus production plotted against recruited biomass from the CRA 3 base case MPD.

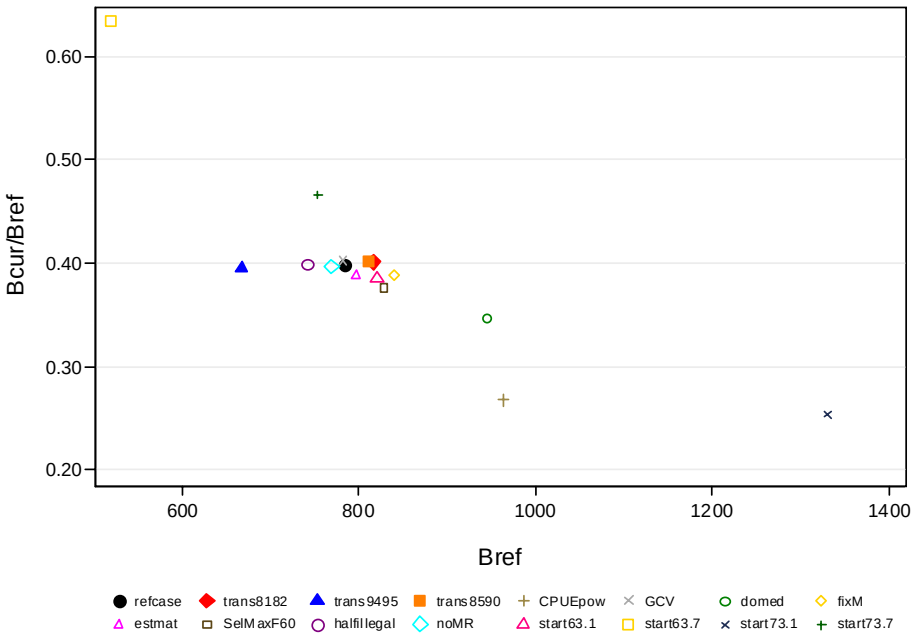

Figure 16. Relationship of *B2008/Bref* relative to *Bref* for the base case and 15 of the MPD sensitivity trials. In this case *Bref* is the mean of AW vulnerable biomass for 1974–79.

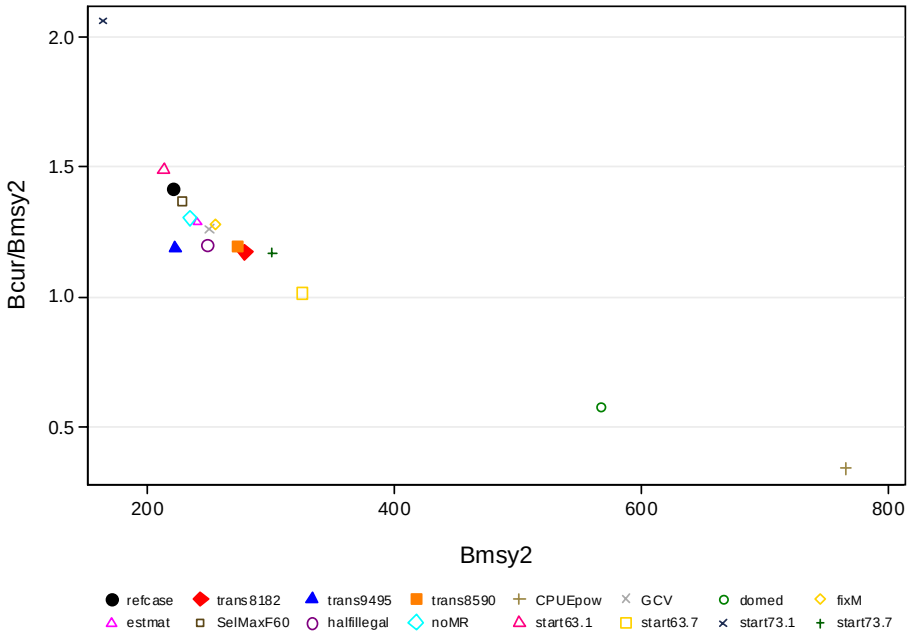

Figure 17. Relationship of *B2008/Bmsy2* relative to *Bmsy2* for the base case and 15 of the MPD sensitivity trials.

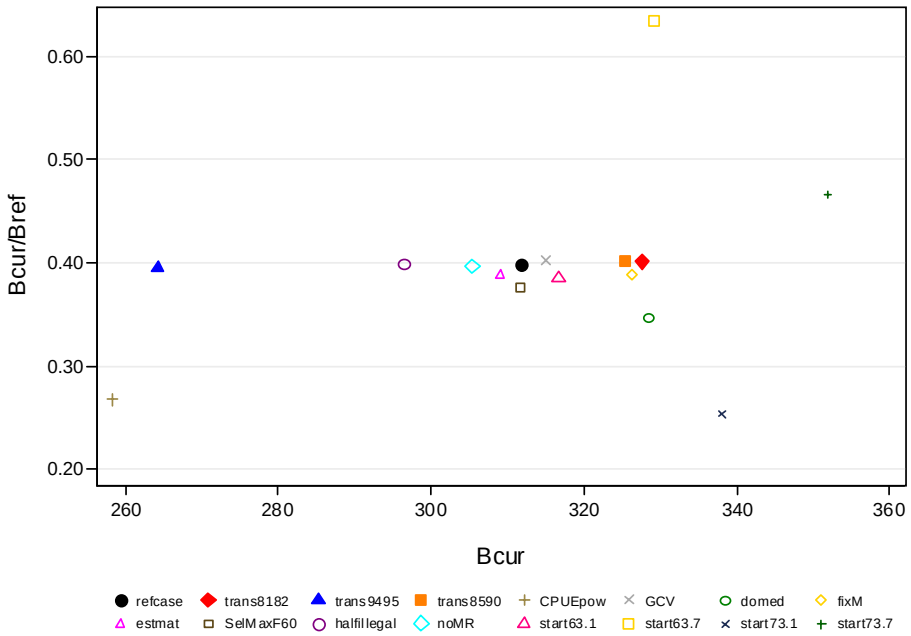

Figure 18. Relationship of *B2008/Bref* relative to *B2008* for the base case and 15 of the MPD sensitivity trials. In this case *Bref* is the mean of AW vulnerable biomass for 1974–79.

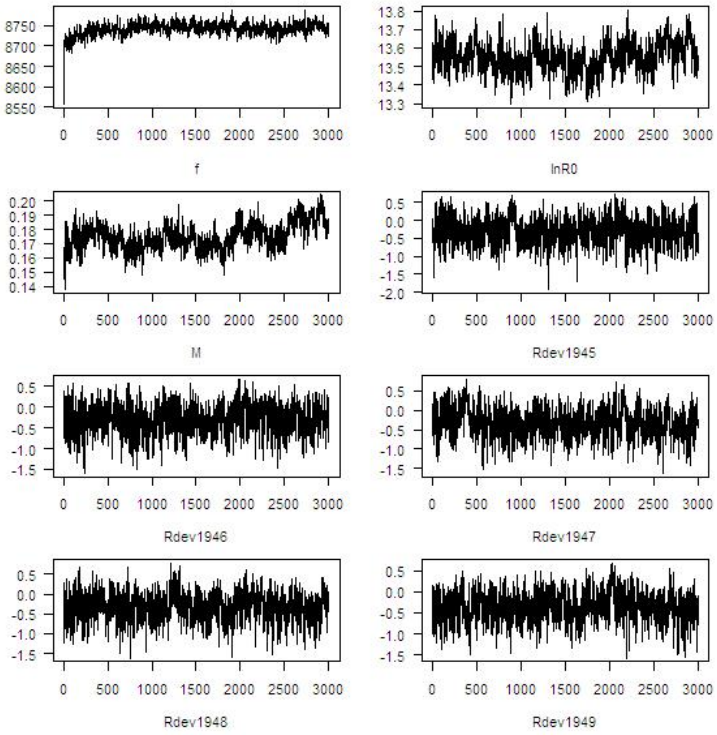

Figure 19: Traces for the total function value (f), *lnR0*, *M* and *Rdevs* for the years indicated.

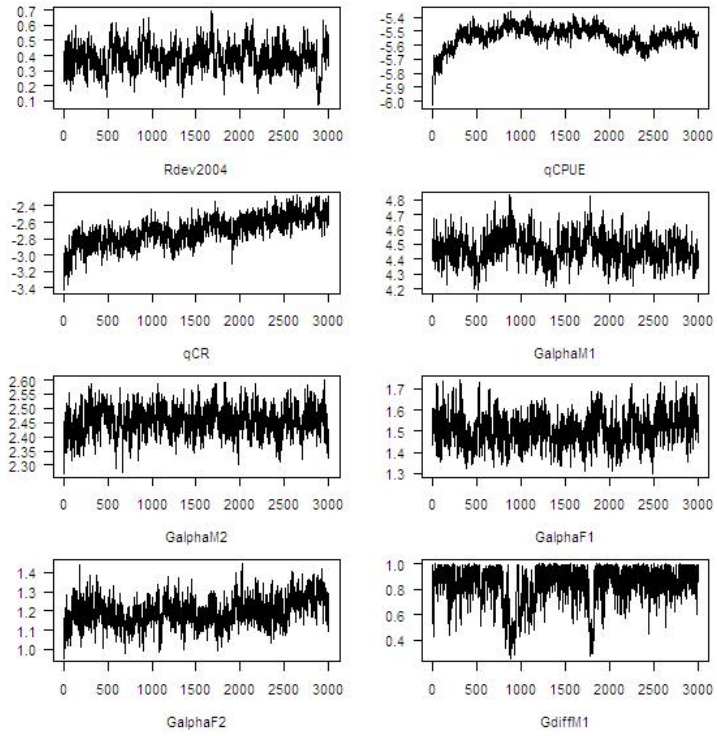

Figure 20: Traces for the 2004 *Rdev*, *lnqCPUE* and *lnqCR*, and the five growth parameters indicated.

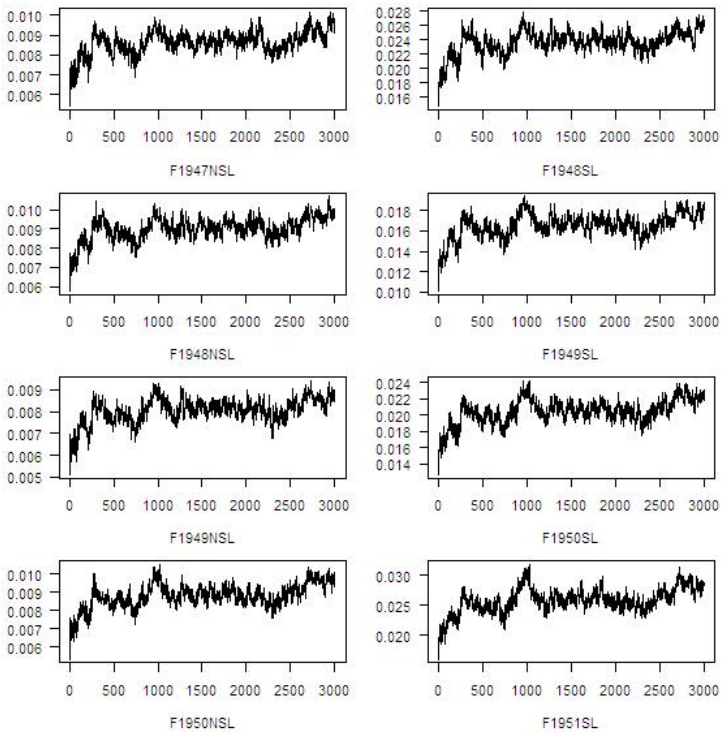

Figure 21: Traces for fishing mortality rates for the NSL (left) and SL fisheries for 1947–51.

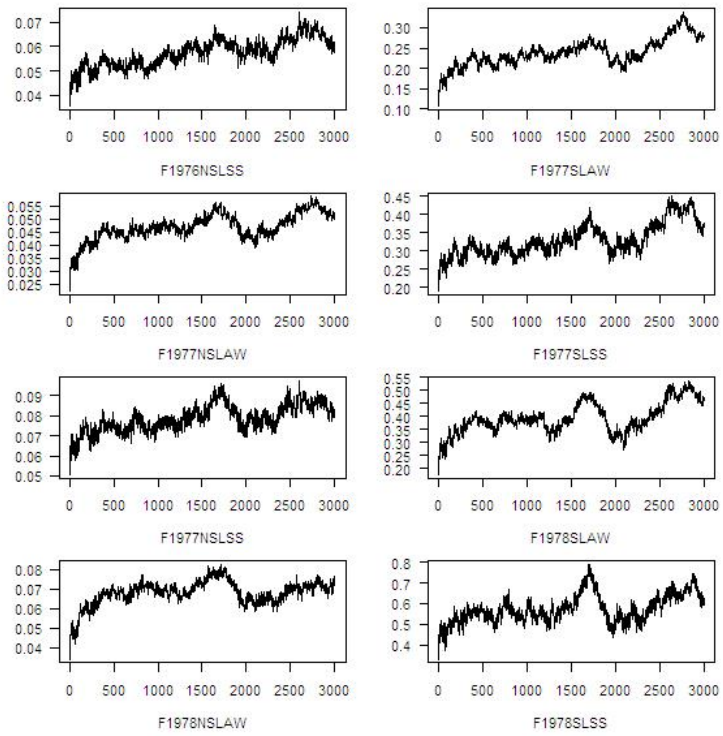

Figure 22: Traces for fishing mortality rates for the NSL and SL fisheries by season from 1976–78.

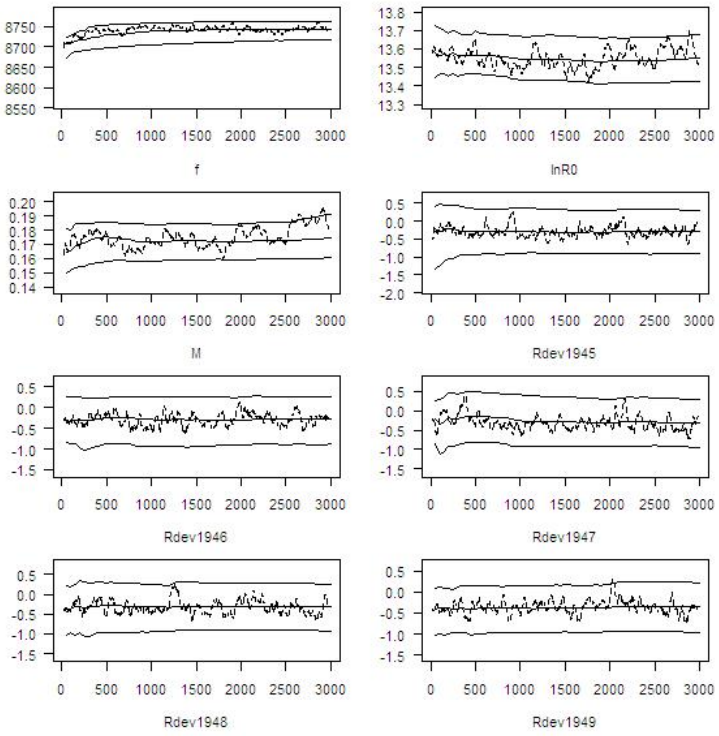

Figure 23: Diagnostic plots for the parameters in Figure 19.

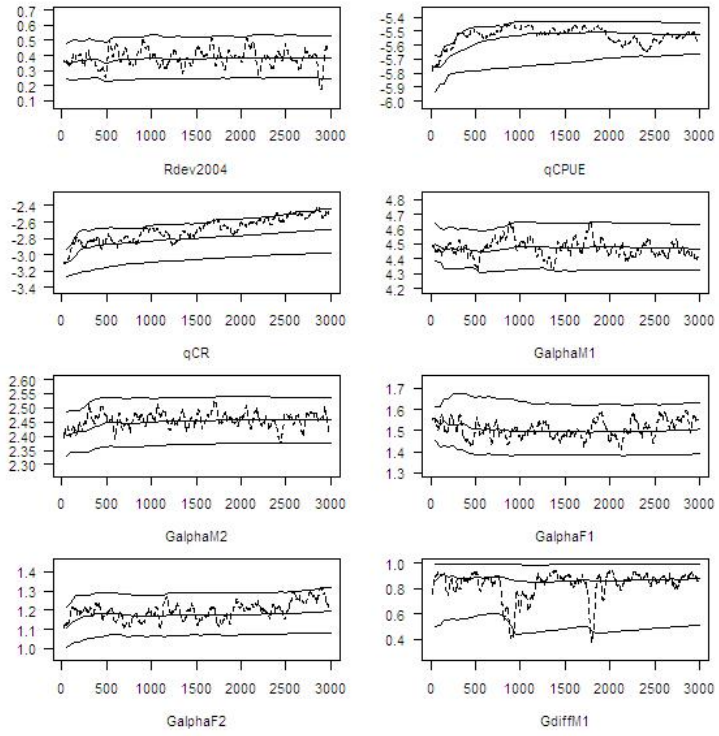

Figure 24: Diagnostic plots for the parameters in Figure 20.

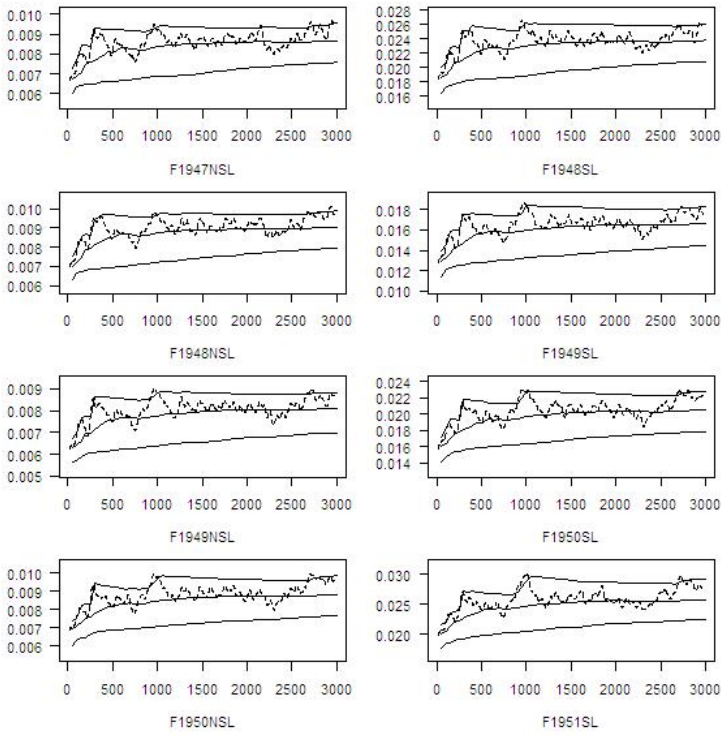

Figure 25: Diagnostic plots for the parameters in Figure 21.

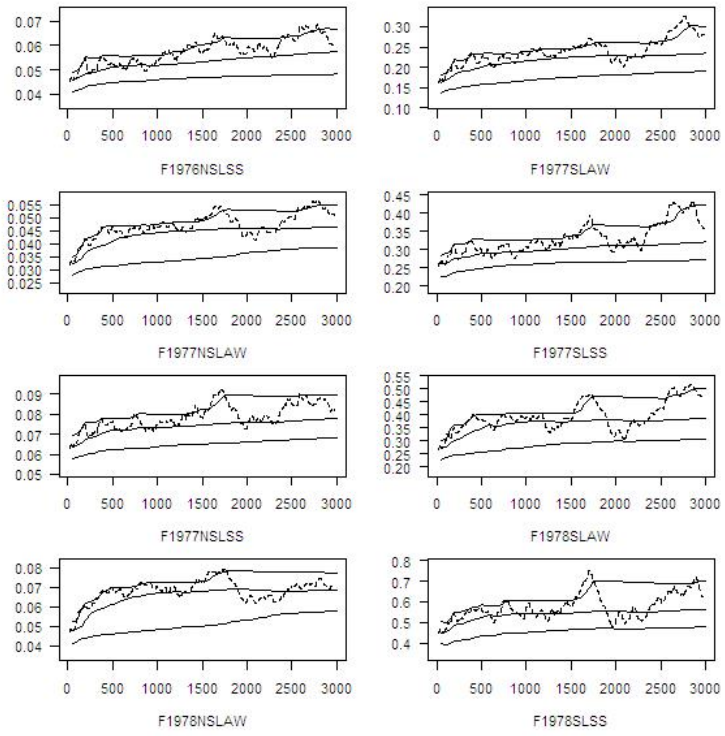

Figure 26: Diagnostic plots for the parameters in Figure 22.

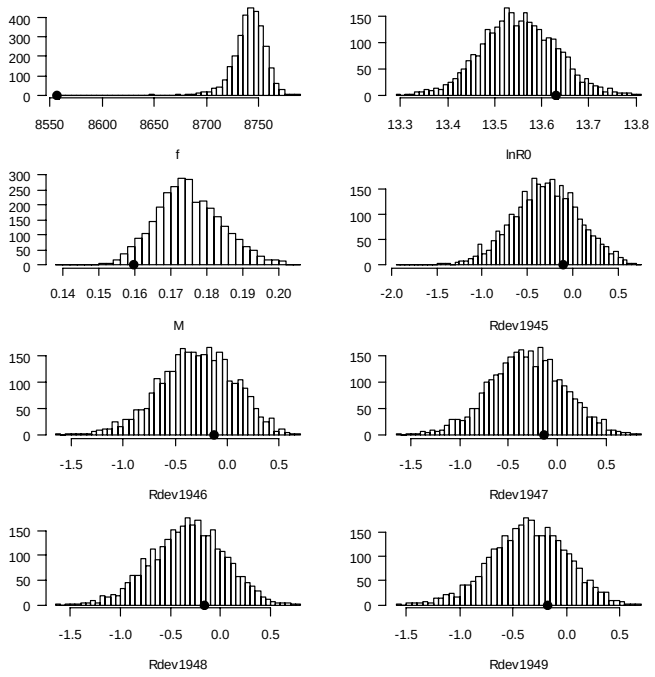

Figure 27: Marginal posterior distributions of the parameters in Figure 19. The small black circle indicates the MPD estimate.

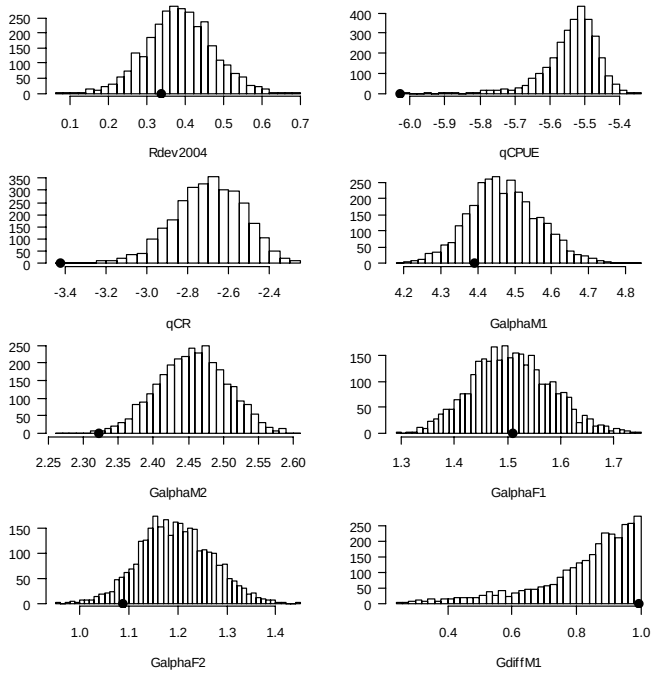

Figure 28: Marginal posterior distributions of the parameters in Figure 20. The small black circle indicates the MPD estimate.

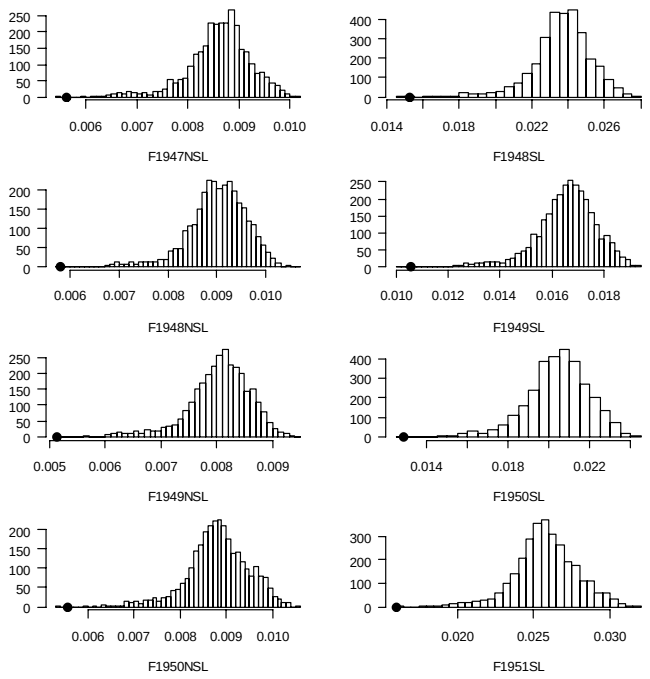

Figure 29: Marginal posterior distributions of the parameters in Figure 21. The small black circle indicates the MPD estimate.

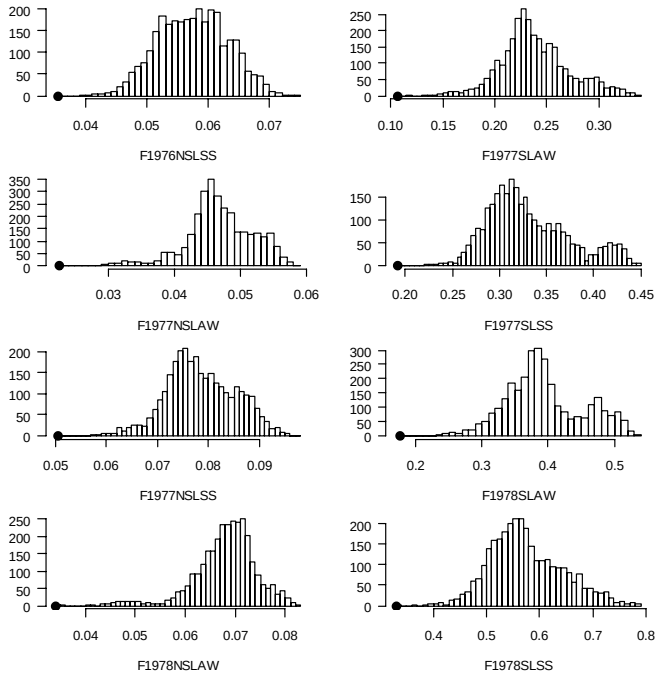

Figure 30: Marginal posterior distributions of the parameters in Figure 22. The small black circle indicates the MPD estimate.

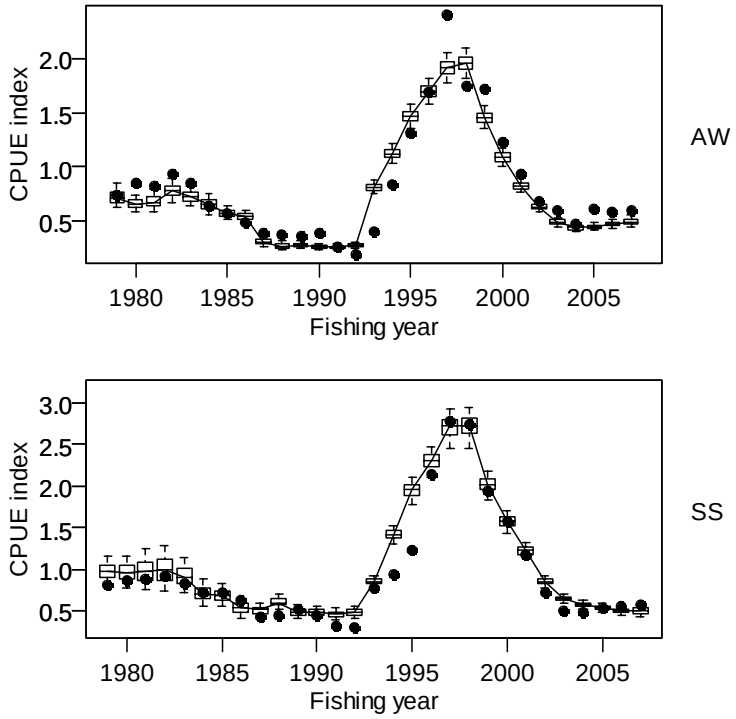

Figure 31: From the CRA 3 base case McMC, the posterior trajectory of observed (black circles) and predicted (box plots) CPUE.

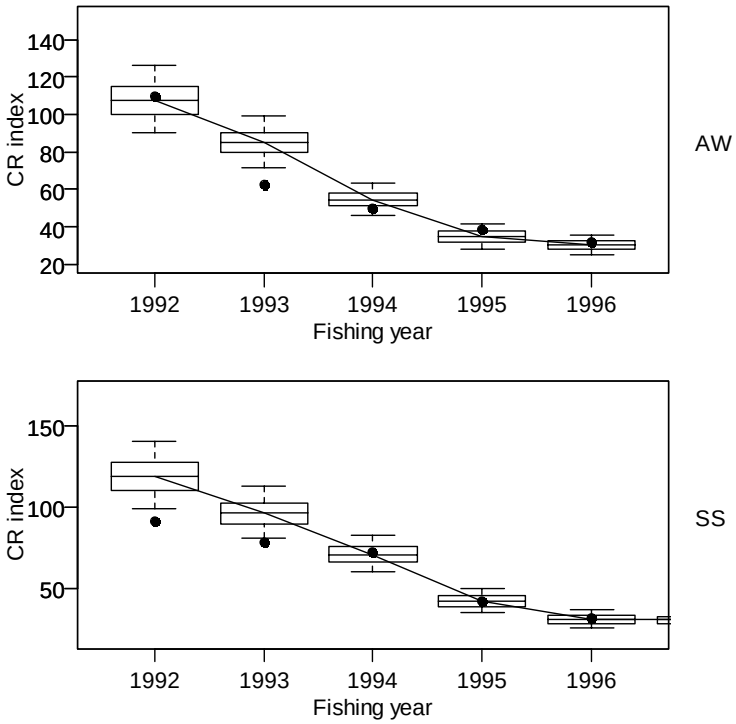

Figure 32: From the CRA 3 base case McMC, the posterior trajectory of observed (black circles) and predicted (box plots) CR.

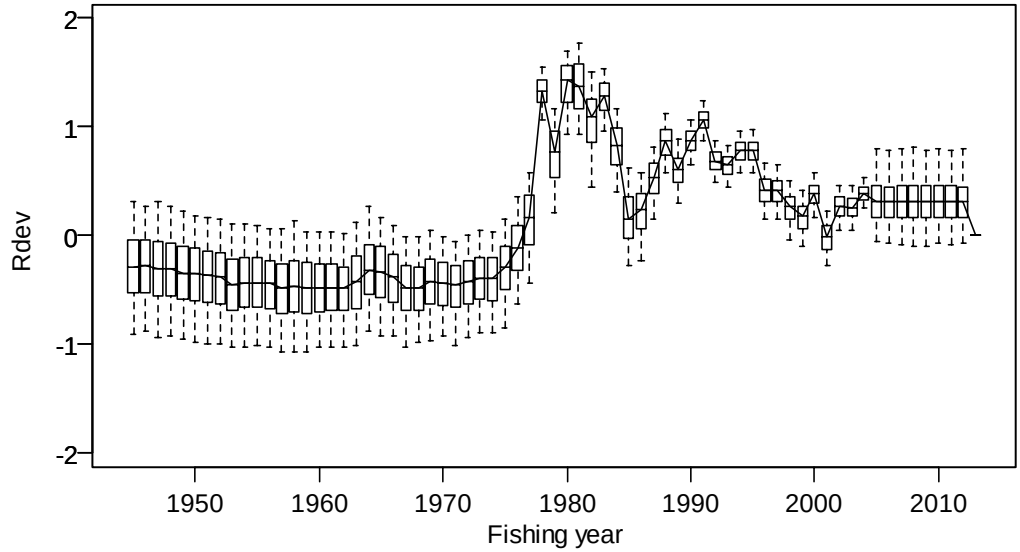

Figure 33: From the CRA 3 base case McMC, the posterior trajectory of *Rdevs*.

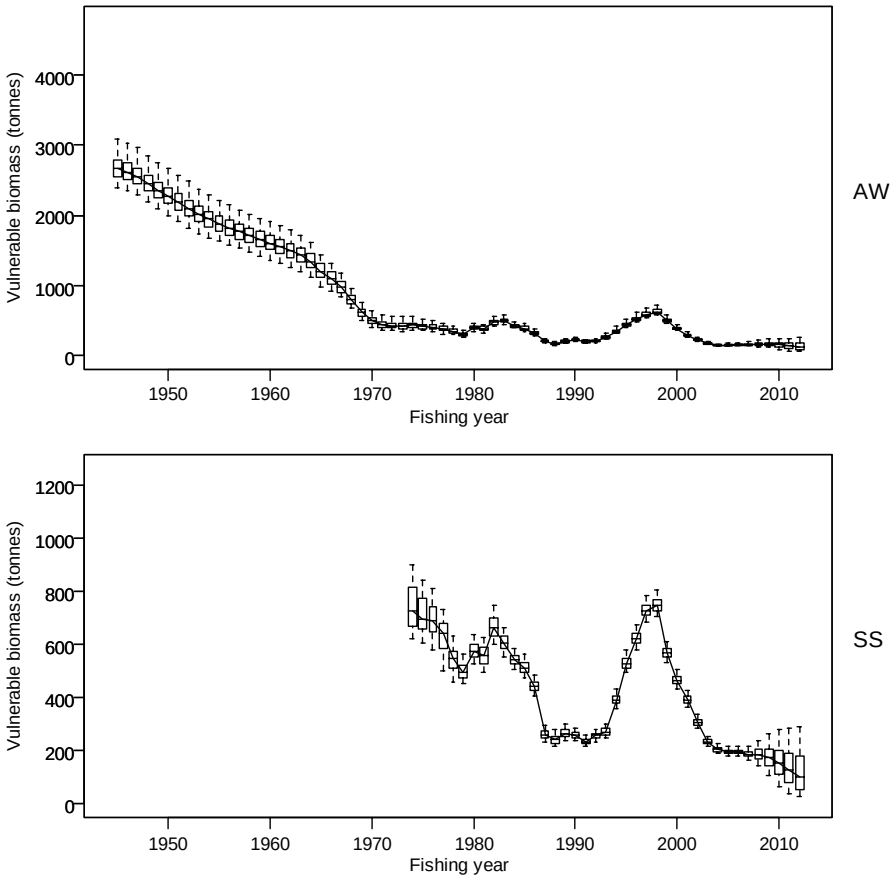

Figure 34: From the CRA 3 base case McMC, the posterior trajectory of vulnerable biomass by season: AW upper.

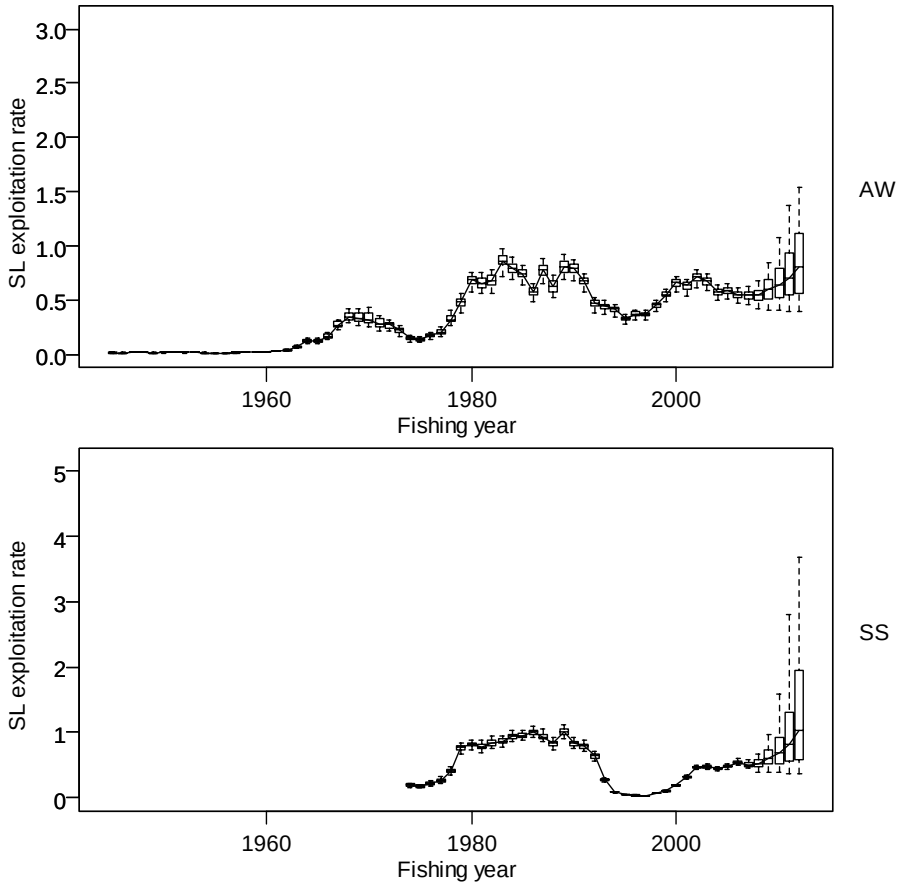

Figure 35: From the CRA 3 base case McMC, the posterior trajectory of SL exploitation rate by season: AW upper.

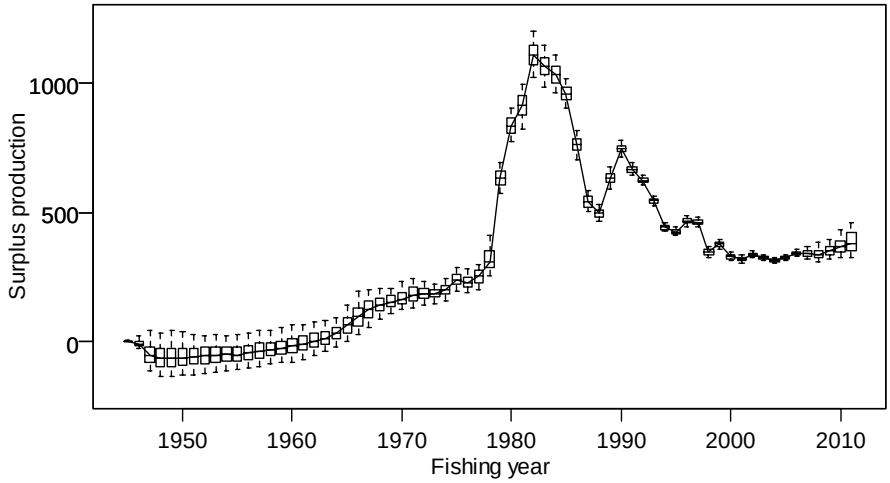

Figure 36: From the CRA 3 base case McMC, the posterior trajectory of surplus production.

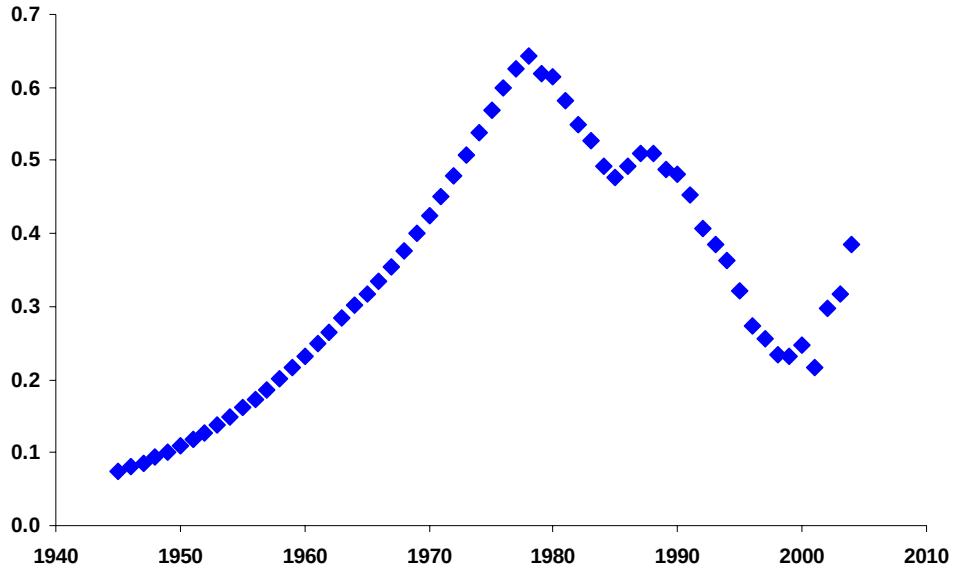

Figure 37: "Backwards-running" mean of *Rdev*s from the base case CRA 3 McMC. The point shown for each year is the average of *Rdev*s from that year through 2004, inclusive.